Reliability Engineering and System Safety 238 (2023) 109489

Contents lists available at ScienceDirect

Reliability Engineering and System Safety

journal homepage: www.elsevier.com/locate/ress

Spatial modeling and analysis based on spatial information of the ship encounters for intelligent navigation safety

Zhichen Liu [a], Ying Li [a,*], Zhaoyi Zhang, Experiments [a,b], Wenbo Yu [c], Yegang Du [d]

[a] Navigation College, Dalian Maritime University, Dalian, Liaoning 116026, China
[b] Department of Engineering Technology, College of Technology, University of Houston, Houston, TX, USA
[c] Northeastern University, Shenyang, Liaoning 110167, China
[d] Future Robotics Organization, Waseda University, Tokyo, Japan

ARTICLE INFO

Keywords:
Intelligent navigation safety
GIS
Spatial modeling analysis
Collision risk
Ship-encounter space domain

ABSTRACT

The analysis of dangerous navigation situations is crucial for the advancement of intelligent shipping technology. In this study, we propose a spatial modeling and analysis method in the space domain of ship encounters based on a geographic information system spatial information platform and analysis technology. The proposed method employs various parameters, such as the approaching rate of a ship, the relative orientation, the encounter danger, the relative spatial position, and the power coefficient of the exponential mathematical curve to establish a dynamic spatial–temporal model of ship encounters. This allows for the spatial modeling and analysis of the spatial characteristics and distributions of encounter-danger surface sources. The proposed method enables in-depth analysis of potential nonlinear spatial characteristics and distribution patterns of ship-encounter danger during navigation and provides spatial analysis results, including encounter-safety features and spatial–temporal attribute information for safe ship navigation. This can greatly improve the spatial analysis and perception ability of ships encountering dangerous situations, thereby effectively reducing the spatial ambiguity of encountering danger. This study performs case analysis and comparative verification using two types of encounter scenarios, and the results reveal the accuracy and superiority of the proposed method.

1. Introduction

1.1. Background

Advancements in maritime transportation have led to an increase in the number of ships, resulting in a higher density of maritime traffic and a yearly increase in maritime traffic accidents [1]. These accidents have caused casualties, property losses, and significant social impacts. According to the European Maritime Casualty Information Platform database, an average of 3239 marine traffic accidents occurred per year from 2011 to 2021 [2]. The European Maritime Safety Agency has recorded the number of accidents in the past seven years (2014–2021) and analyzed their causes, as illustrated in Figs. 1 and 2 [2]. The agency's records determine the probability of avoiding ship collisions and contain a large amount of marine accident data. According to the results, the proportion of maritime accidents caused by ship collisions exceeds 50%. Examples of such accidents include the continuous collision of the upward seagoing ship Guoyuan 1 and the collision and explosion of the Sanchi ship. Ship collisions not only lead to serious casualties and property damage but also have a negative impact on society. Fig. 3 presents a map of the global maritime accident density, which is based on maritime accident data published by the Global Integrated Shipping Information System and provided by the International Maritime Organization (IMO). We use the uniform sampling method to divide the world map into 30 × 60 grids (i.e., each grid has a latitude and longitude length of 6°) for density value normalization spatial processing. As shown in Fig. 3, the redder the sea area, the greater the density of maritime accidents. This map reveals clusters of high-severity accidents

Abbreviations: ALARP, as low as reasonably practicable; ARPA, automatic radar plotting aid; COLREGS, convention on the international regulations for preventing collisions at sea; CRI, collision risk index; DCPA, distance at closest point of approach; GIS, geographic information system; GISIS, Global Integrated Shipping Information System; IMO, International Maritime Organization; MAE, Mean absolute error; RE, Mean relative error; NN, Natural neighbor; RMSE, Root-mean-square error; TCPA, Time to closest point of approach.

* Corresponding author.
E-mail address: zhichen@dlmu.edu.cn (Y. Li).

https://doi.org/10.1016/j.ress.2023.109489
Received 12 August 2022; Received in revised form 24 June 2023; Accepted 29 June 2023
Available online 30 June 2023

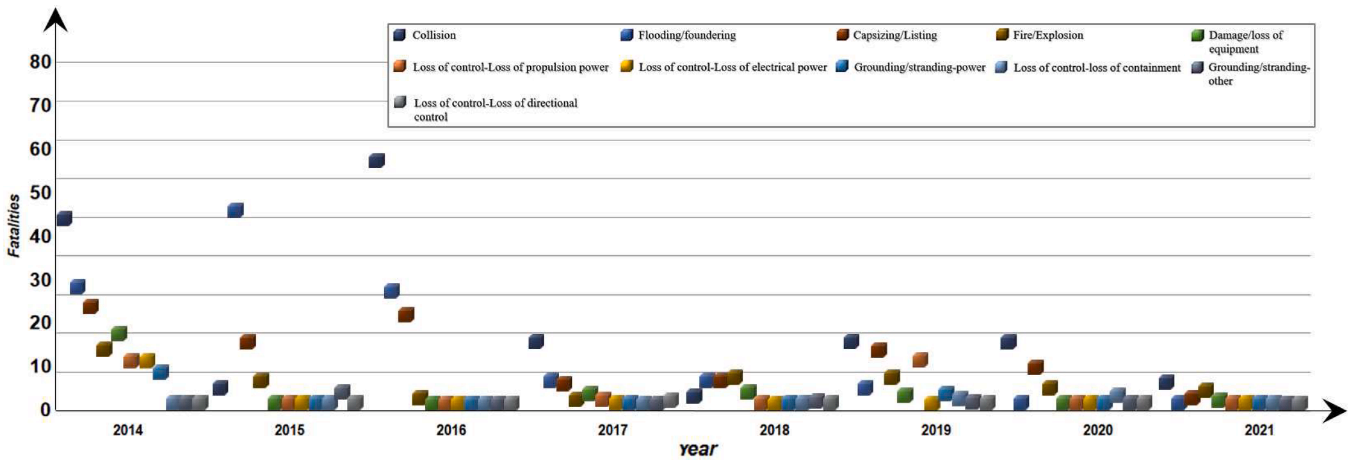

Fig. 1. Histogram of the numerical distribution of maritime accidents during 2014–2021 based on the accident type (source: European Maritime Safety Agency, 2022 [2]).

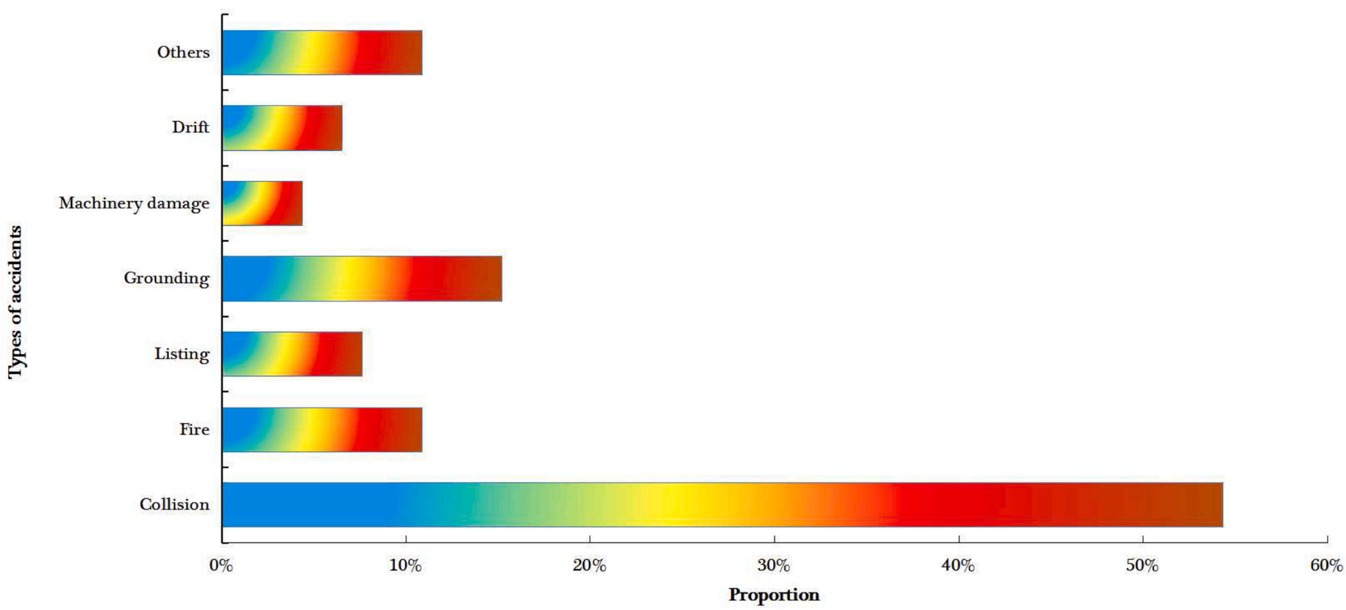

Fig. 2. Numerical analysis of the causes of maritime accidents during 2014–2021 (source: European Maritime Safety Agency, 2022 [2]).

in coastal areas, such as Vietnam, the Philippine Islands, the Straits of Singapore and Malacca, and the surrounding waters of China, Japan, and South Korea. Lower-density maritime accident clusters occur in the North Sea, Baltic Sea, and Mediterranean Sea. Therefore, there is a need for analysis and perception methods to determine the spatial characteristics of navigation safety in the context of unmanned and intelligent ships. The progress of intelligent maritime traffic safety is vital for human safety, marine environment protection, and the global economic situation, which has gained attention from scientists worldwide.

1.2. Literature review

The IMO has developed and improved several international conventions and rules to improve maritime traffic safety in the 21st century. The formal safety assessment method issued by the IMO [3,4] is widely adopted by most countries to evaluate the safety index of maritime navigation and promote the research and development of navigation risk analysis methods. Based on the research progress of early scholars, Coldwell proposed a ship domain model for restricted waters and explained its application in the buoyed channel [5]. Zhao et al. reported a method for analyzing the influencing factors of the ship domain based on the theory of proxemics [6]. Wu and Zheng established a time collision risk model based on the stimulus perception theory and explained the physical significance of time collision risk [7]. Moreover, researchers have achieved significant progress in the safety of ship encounters through literature surveys. The distance at the closest point of approach (DCPA) and the time to the closest point of approach (TCPA) are currently the primary methods to avoid ship collisions and develop decision support systems. They are characterized by their simplicity and clear calculation. In a quantitative study of ship collision risk, Kearon proposed a method for evaluating collision risk by calculating the weights of the DCPA and TCPA [8]. Subsequently, collision risk assessment was performed using automatic information system data of the Yangtze River in China by combining the distance and relative velocity between ships to exploit the advantages of DCPA and TCPA [9]. This collision risk assessment is suitable for multiship-encounter scenarios [10,11]. Liu et al. proposed a spatial analysis model for collision risk analysis of multiship-encounter situations based on the closest point of approach using a geographic information system (GIS) platform [12]. This model accurately represents ship maneuvering and has been widely

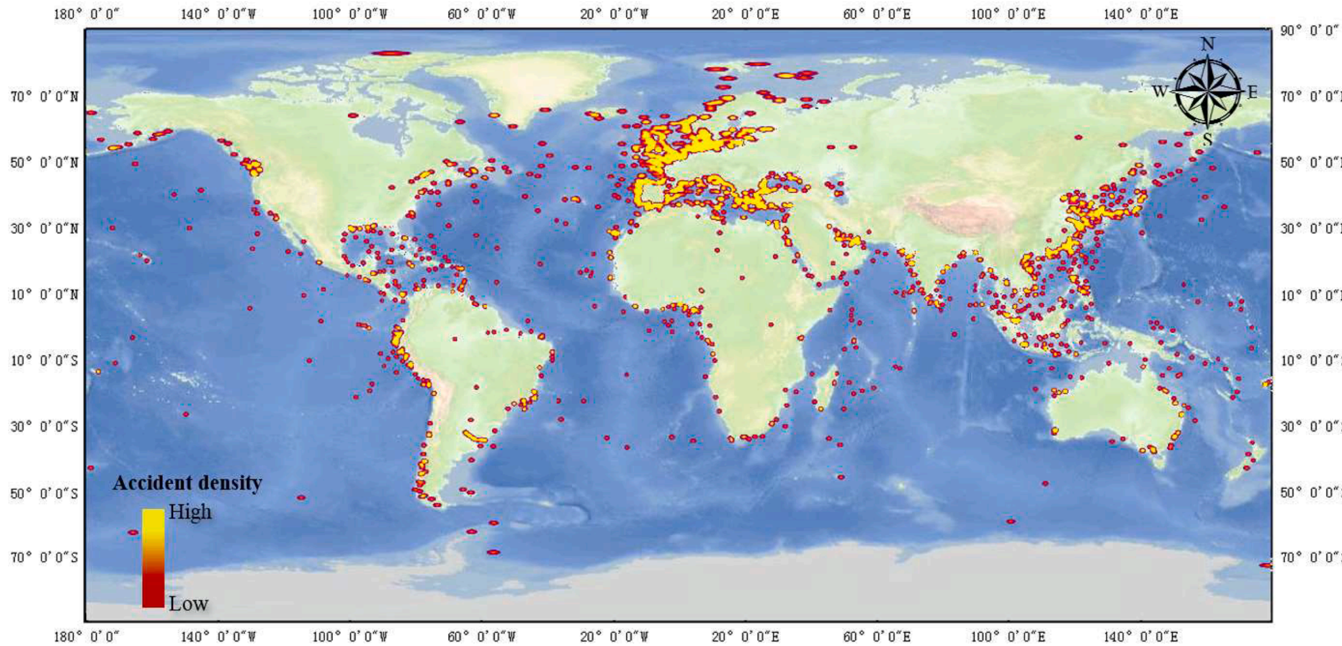

Fig. 3. Map of global maritime accident density (source: Global Integrated Shipping Information System).

used in the transportation industry. However, during the hazard analysis of complex ship-encounter scenarios, relying solely on the DCPA and TCPA may not accurately identify hazards at sea. As a result, ship domain theories have been proposed [13,14].

The ship domain model is a safe-encounter-distance model that considers factors such as ship size, motion parameters, and encounter situations [15–19]. Unlike the circular area developed using the DCPA, the safe encounter distance of target ships may differ in different directions. However, there is currently no unified calculation method for the ship domain model, and there is a theoretical gap in visually representing the relationship between the perception of the nonlinear spatial feature of ship encounters and the spatial representation of information on ship-encounter hazards. To address this gap, the concept of a ship-encounter hazard water area, which reflects the refined perception and spatial representation of the ship-encounter hazard space, is applied to an automatic radar plotting aid (ARPA) to transform the navigation danger from a point range to an area range. However, the full utilization of spatial perception is restricted due to the limitations of ARPA, such as its low ability for vector display.

With the development of computer vision modeling, the spatial representation of ship collision risk has attracted research attention. For example, Imazu et al. visualized ship collision risk based on the target obstacle detection method; however, the circular-area model they used could not fully determine the probability of avoiding ship collisions [20]. The ship domain model and critical safety area have been used to quantify the risk of collisions between ships and stationary obstacles and to guide collision avoidance, thereby promoting the safety of intelligent navigation [21]. The concept of dynamic boundaries, originally proposed by Davis, refers to a super-domain space where the driver takes urgent action to avoid a collision [22]. This space requires further investigation to reflect the anisotropy of safety distance and the spatial variability of collision risks.

Additionally, in recent years, many scholars and experts have used various intelligent algorithms, information technology, and other emerging methods for conducting in-depth research on the identification and analysis of ship navigation safety and encounter hazards to promote scientific and technological levels of intelligent navigation technology research. Pietrzykowski and Uriasz studied the dynamic changes in ship navigation encounters in open water [23]. Pietrzykowski combined artificial intelligence methods, integrated AIS, ENC, ARPA, GNSS, and other multisource navigation information, intelligently learned the knowledge of safe navigation, and developed a navigation decision support system (NAVDEC) [24,25]. Wang S et al. proposed an adaptive model for the multiship-encounter situation [26], thereby predicting the navigation intention of the target ship and assisting safe encounters. These algorithms have generally achieved good results in calculating ship navigation risk prediction. Lijia Chen [27,28] conducted gray-box identification modeling on the internal laws of ship maneuvering motion and deeply studied the MASS maneuvering motion prediction problem, effectively promoting the technical level of intelligent ship motion modeling. Scholars from Aalto University, a leading Scandinavian institution of higher learning, have provided insights into the development of research in the field of marine engineering over the past 50 years. The importance of new technologies, such as machine learning and neural networks, was explored, and the path forward in the field of ship navigation technology was studied [29]. Moreover, a new method that combines knowledge derived from big data analytics was released to achieve collision probability estimation and assess ship damage risk after collision events [30]. Furthermore, we conducted an in-depth study and summarized the research work in the field of typical ship navigation safety and risk analysis in recent years and elaborated on the development trend characteristics and methods of applying this typical research work. Table 1 presents the detail of the development trends in the field of ship navigation safety and risk analysis in recent years. Most of these research cases mainly use ship elliptic domain, big data analysis, machine learning method, and Bayesian network, among other techniques, to perform risk prediction and analysis in the aspect of navigation safety analysis. These cases achieved excellent application results and values. Moreover, the methods they proposed are highly feasible and accurate, can greatly improve navigation safety analysis ability, and provide forward-looking method support and reference value for the development of intelligent navigation situational safety awareness theory. Moreover, the results show a clear and strong trend of navigation safety analysis technology becoming one of the core technologies for intelligent navigation.

In summary, many research institutions have invested their efforts in researching navigation safety situation analysis technology and have achieved good results. The analysis and acquisition methods of

Table 1
Research history and development trends in the field of ship navigation safety and encounter-hazard identification and analysis in recent years.

Literature	Application method or main content	Literature	Application method or main content
Goerlandt and Montewka (2015) [31]	Summarized the main achievements of risk definition and risk analysis for ship navigation, focusing on the application of solving maritime accident risks.	Murray and Perera (2021) [46]	Proposed a deep learning framework to predict ship navigation trajectories using AIS data, providing information support for navigation safety.
Goerlandt et al. (2015) [32]	Proposed a framework for risk-informed maritime CAS (RICAS), which applies to case studies of open sea navigation. The performance of this method has been improved by comparison.	Zhang et al. (2021) [47]	Proposed a big data analysis method for evaluating ship–ship collision risk information based on AIS data and nowcast data.
Varas et al. (2017) [33]	Deeply discussed Machine Executable Collision Regulations for Marine Autonomous Systems (MAXCMAS) and developed a path planner that complies with COLREGs for autonomous ship navigation.	Li et al. (2021) [48]	Proposed a practical rule-aware time-varying conflict risk measure method, enabling real-time risk assessment of ship collisions and assessment of collision hazards between multiple ships.
Tian et al. (2018) [34]	Proposed a very innovative approach, which successfully implements risk assessment of nautical navigational environment based on a risk cloud model and verifies the superiority of the method by comparing it with traditional methods.	Zhu et al. (2021) [49]	Proposed a method based on neural networks that is used to establish a domain model that considers the effects of visibility and maneuverability. The analysis of danger encountered by ships within a certain range was realized.
Chen et al. (2019) [35]	Summarized the advantages and disadvantages of typical methods for ship collision risk assessment and proposed a classification mode based on the technical characteristics of ship collision risk assessment methods.	Zhang et al. (2022) [50]	Successfully implemented the evaluation of grounding risk under real environmental conditions using the newly proposed machine learning method for big data analysis.
Gil et al. (2020) [36]	Constructed a novel safety maneuvering zone for onboard decision support systems when two ships encounter based on the proposed new concept of Collision Avoidance Dynamic Critical Area.	Montewka et al. (2022) [51]	Investigated a method that can effectively evaluate the accident susceptibility of maritime vessels, greatly improving the crew's situational awareness.
Zhang et al. (2020) [37]	Proposed a ship collision risk classification model based on convolutional neural networks.	Zhang et al. (2022) [52]	Proposed an improved approach for the maritime traffic flow complexity estimation in inland waterways for traffic safety management.
Du et al. (2020) [38]	Conducted a critical review of maritime waterway safety assessment methods based on nonaccident critical events detected using AIS data.	Kim et al. (2022) [53]	Published ship–ship collision and grounding benchmarks for structural response analysis of ships and validated simulations of typical accident scenarios.
Dinis et al. (2020) [39]	Proposed a probabilistic approach for characterizing the static risk of ships using Bayesian networks to realize the analysis and assessment of ship navigation risk profile.	Xu et al. (2022) [54]	Studied a Bayesian network model considering human factors and operational factors, which are to predict the probability of ship besetting in ice during convoy operations along the Northern Sea Route.
Liu et al. (2021) [40]	Used GIS spatial logic model to extract spatial features of encountering danger and solve the safety problem of ship encountering space.	Mazurek et al. (2022) [55]	Proposed a novel framework for estimating the likelihood of a ship–ship collision and identifying collision-prone locations. The result accuracy increased by 16% compared to the traditional model.
Abaei et al. (2021) [41]	Used hierarchical Bayesian inference to predict the safety factor of the entire system during the safe navigation process of intelligent ships.	Antão et al. (2023) [56]	Combined the Cox proportional hazard regression model and Bayesian rule to assess the factors influencing ship collision risk.
Yu et al. (2021) [42]	Proposed a multidata-driven framework for ship navigation risk assessment and used a hybrid method to successfully evaluate the static and dynamic risks of ship navigation.	Zhang et al. (2023) [57]	Proposed an interpretable knowledge-based decision support method based on AIS data, thus successfully planning a safe route to avoid collisions.
Silveira et al. (2021) [43]	Used the standards related to ship motion, ship characteristics, and environmental factors and then used the ELECTRE Tri-nC multicriteria super-level method to evaluate the risk of ship collision.	Liu et al. (2023) [58]	Proposed novel multisensor data fusion algorithms, which utilize an unscented Kalman filter to improve the accuracy of USV navigation data and the accuracy of ship navigation.
Zhang et al. (2022) [44]	Used the knowledge-based decision support method to construct a two-stage collision avoidance behavior extraction algorithm based on AIS data, which successfully achieved ship collision avoidance.	Zhang et al. (2023) [59]	Proposed a novel deep learning method that can successfully achieve the prediction of Six degrees-of-freedom ship motion dynamics.
He et al. (2022) [45]	Proposed an open-water intelligent navigation decision-making method that can dynamically adapt to the residual error in the system and the target ship's	Zhang et al. (2023) [60]	Actively developed an autonomous navigation safety auxiliary module based on INS/GNSS onboard, and its effectiveness was verified through actual

(continued on next page)

Table 1 (*continued*)

Literature	Application method or main content	Literature	Application method or main content
	random manipulation.		ship experimental data validation.

nonlinear spatial distribution rules and spatial variation trends in the ship-encounter space domain have not been thoroughly explored. Therefore, in this study, we developed a GIS-based spatial modeling and analysis method based on the ship-encounter space domain and performed spatial modeling analysis of the potential danger trends in this domain based on multiple spatial–temporal parameters. This method enables in-depth analysis and perception of potential nonlinear spatial characteristics and distribution patterns of ship-encounter danger during ship navigation. As a result, the spatial analysis and perception ability of ships encountering danger are greatly improved, and the spatial ambiguity of encountered dangers is greatly reduced.

The remainder of this paper is organized as follows. Based on the background and literature review presented in Section 1, Section 2 describes the current challenges in navigation-encounter danger analysis and presents the aims of this study. Moreover, it discusses the scientific innovation and potential of GIS spatial analysis for ship-encounter safety. Section 3 describes the proposed spatial modeling and analysis method for the ship-encounter space domain. Section 4 presents practical examples of ship-encounter scenarios to illustrate the effectiveness of the proposed method. It also includes a comparative analysis of accuracy to evaluate the proposed method and discusses the simulation results and method in detail. Section 5 concludes the paper and proposes directions for future research.

2. Research goals

The literature review and analysis presented in Section 1 highlight the challenges in analyzing the spatial characteristics and distribution of ship encounters, which have been a significant problem in ship-encounter danger perception and a bottleneck in intelligent navigation research. Most existing ship-encounter danger assessment algorithms focus on the numerical analysis of collision risks; however, there has been a lack of in-depth analysis of the nonlinear spatial characteristics and distribution of ships encountering dangers. Furthermore, the ship-encounter danger is a spatial–temporal attribute closely related to the time and space position of the ship, resulting in complex interconnected spatial–temporal differences and numerous potential nonlinear spatial characteristics and distributions.

When a ship encounters complex waters, such as turning routes, multiple obstacles, and dense waters, unknown nonlinear spatial characteristics and distribution patterns are observed regarding the dangers encountered by the ship in each spatial–temporal state. Ships have complex characteristics, such as coexisting dynamic and static characteristics and a discrete distribution in space and time while sailing. Therefore, to determine the nonlinear spatial characteristics and distribution patterns of the nonlinear ship-encounter space domain and address the challenge of visually presenting the relationship between the refined perception and spatial representation of ship-encounter danger, in this study, we investigate the theory and method of spatial analysis of ship-encounter danger based on a spatial information platform. Additionally, we propose a method based on GIS spatial modeling and analysis of the ship-encounter space domain to solve the research problems described above. The proposed method leverages the high spatial resolution, spatial distribution patterns analysis, and spatial features of the spatial information platform. It uses navigation spatial information data with spatial location, spatial–temporal distributions, and proximity and orientation relations to realize very complex spatial analyses of the accurate extraction and quantification of spatial characteristics of dynamic and static targets for different time series through geometric analysis and advanced spatial calculations.

Currently, few studies have been reported on maritime safety science based on spatial information platforms. However, there is an urgent need to develop spatial analysis methods to calculate ship-encounter hazard characteristics and improve the accuracy of the analysis and perception of the spatial characteristics and distribution of ships encountering dangers of dynamic and static spatial targets during navigation. These methods can achieve spatial analysis of ship-encounter

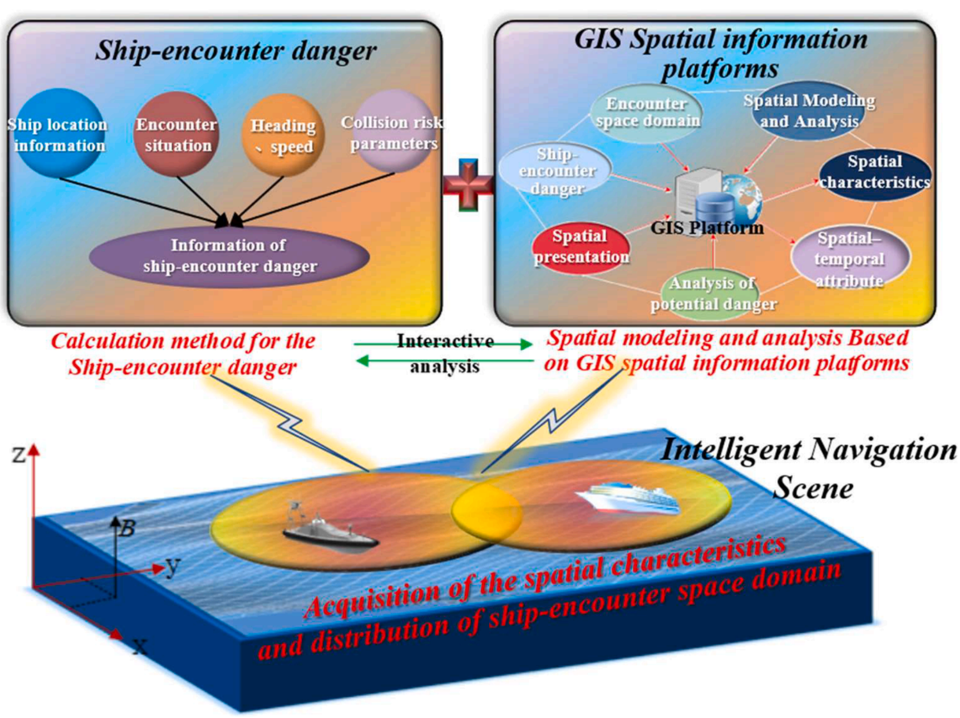

Fig. 4. Framework of the spatial modeling and analysis method proposed in this study.

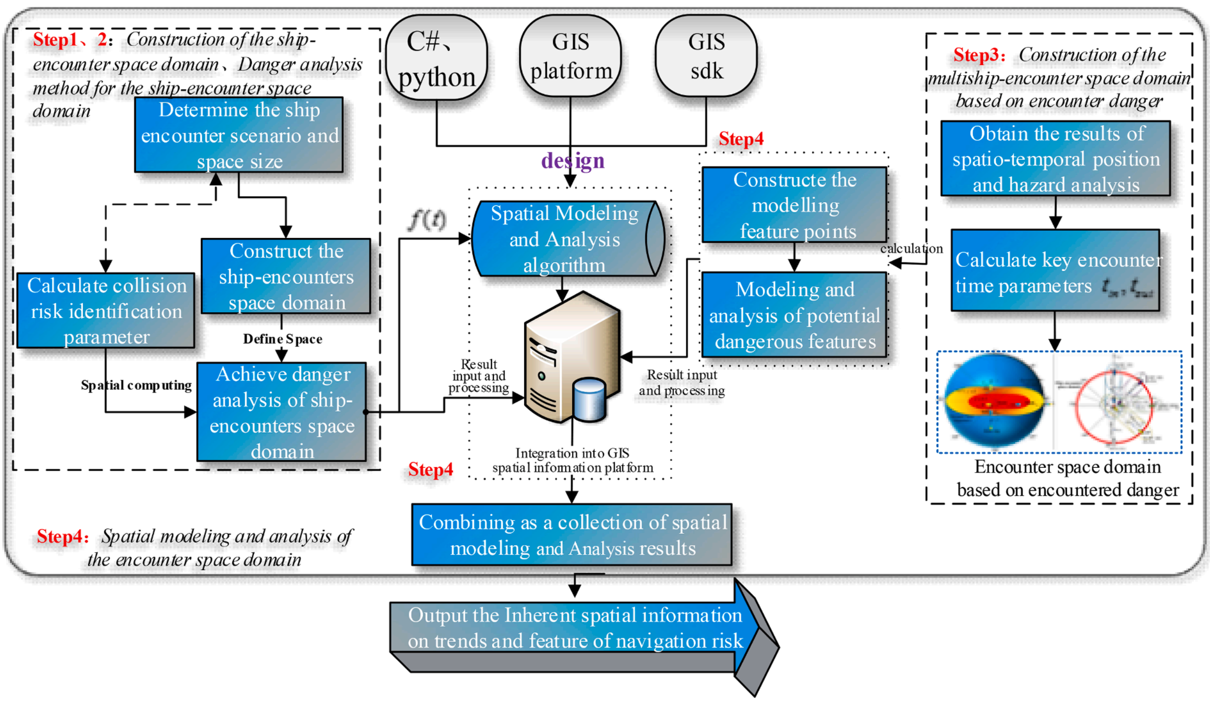

Fig. 5. Specific steps of the proposed spatial modeling and analysis method.

danger and spatial characteristic laws in a multitemporal sequence and nonlinear space, thereby reducing the spatial ambiguity of ship-encounter danger. This study promotes the theoretical innovation of the proposed method for ship-encounter danger analysis based on a spatial information platform and provides theoretical and methodological support for developing intelligent navigation safety systems.

Based on the scientific theory of GIS spatial modeling and analysis, the proposed method can perform in-depth spatial analysis of ship-encounter danger and spatial characteristic information in multi-temporal sequences and nonlinear spaces. The proposed method is based on the approaching rate, identification parameters, relative spatial position distribution, and ship parameters, combined with the power coefficient of the exponential curve, to perform modeling analysis and calculation of the ship-encounter space domain. Using this method, spatial modeling analysis of the potential danger trends in the ship-encounter space domain can be performed and the nonlinear spatial characteristics and distribution in the set of all locations in the ship-encounter space domain can be extracted in a continuous spatial–temporal manner. The proposed method greatly improves the spatial analysis and perception ability of ships in danger, effectively reduces the spatial ambiguity of ship-encounter danger, and enables accurate spatial analysis of multiship-encounter safety. The proposed method was tested using a simulated encounter scenario and exhibited excellent accuracy (97%). The research framework of the spatial modeling and analysis method for the ship-encounter space domain is presented in Fig. 4.

3. Methodology

This section describes the spatial modeling and analysis method for the ship-encounter space domain. This method is mainly divided into four steps. Step I involves the construction of the ship-encounter space domain, Step II is the hazard analysis method of ship-encounter space domain, Step III involves the construction of the multiship-encounter space domain based on encounter danger, Step IV includes the spatial modeling and analysis of the encounter space domain. We describe the specifically developed and used processes of these four key steps in detail in Fig. 5. Next, this section will describe the proposed method in

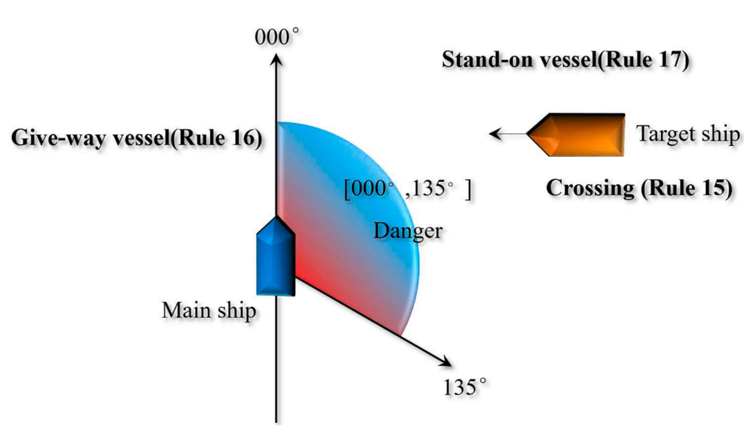

Fig. 6. Graphical expression of vigilance for incoming starboard ships in the Convention on the International Regulations for Preventing Collisions at Sea clauses 15–17.

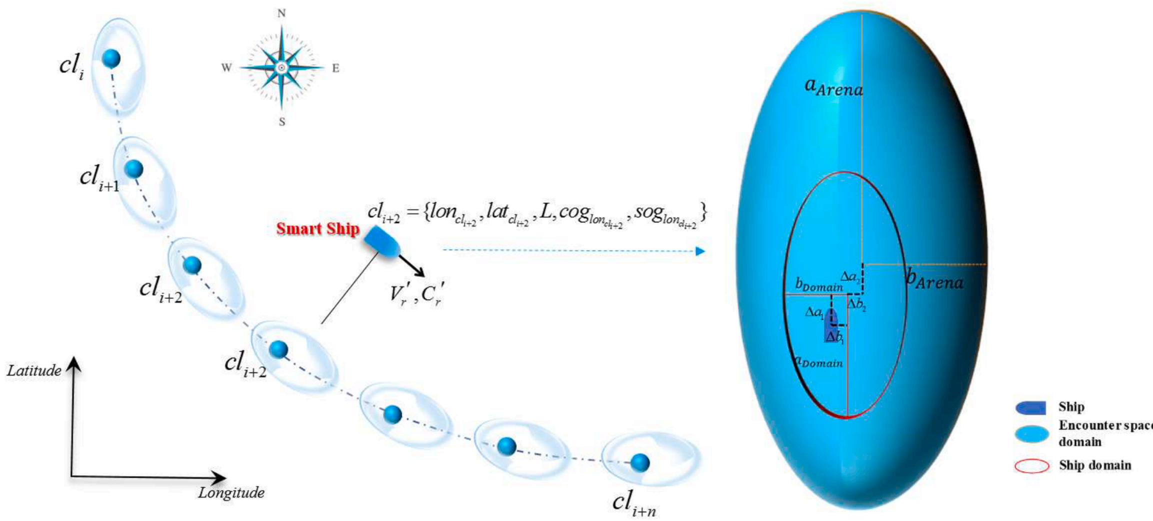

Fig. 7. Detailed construction principle of the ship-encounter space domain during intelligent navigation motion (L is the length of the target ship).

detail in the form of subsections.

3.1. Construction of the ship-encounter space domain

In this study, we first determined the ship-encounter space domain. During a ship's voyage, there are certain space restrictions on the navigation of the ship within the established ship-encounter space domain. Different spatial locations within the ship-encounter space domain have varying risk distributions. The ship-encounter space domain is modeled as an elliptical domain, inspired by the study conducted by Szlapczynski and Szlapczynska [61]. The ship position is placed in the lower left quarter of the center of the offset ellipse, which meets the requirements of enhancing vigilance in the starboard and head-on situations as mentioned in the Convention on the International Regulations for Preventing Collisions at Sea (COLREGs) and reflects the perception of collision risk by ship drivers. Fig. 6 illustrates the clauses in COLREGs that require vigilance during ship sailing. The oval area displayed in Fig. 7 indicates the location where other ships are prohibited from entering, and the collision risk index (CRI) in that space is set to 1.

We studied the spatial distribution of the collision risk between the main ship and the target ship in dangerous waters, which refers to the area where a ship must be aware of a target ship. The CRI is set to 0 at the space boundary of the dangerous water area, also known as the CRI zero boundary. Based on numerous investigations and statistics, Zheng and Wu found that the CRI zero boundary is approximately twice as large as that of the DCPA [62]. Therefore, the dangerous water area should be twice the size of the oval space. Following the safety analysis theory described above, we established the spatial range of waters where ships encounter danger. This spatial range can ensure that the relative position of the ship and the center of the ship domain remain unchanged to facilitate accurate calculation of the risk degree in accordance with the collision avoidance rules specified in COLREG clauses 15–17 (Fig. 6). Fig. 7 presents the detailed construction principle of the ship-encounter space domain during navigation. The displacement of a ship along the

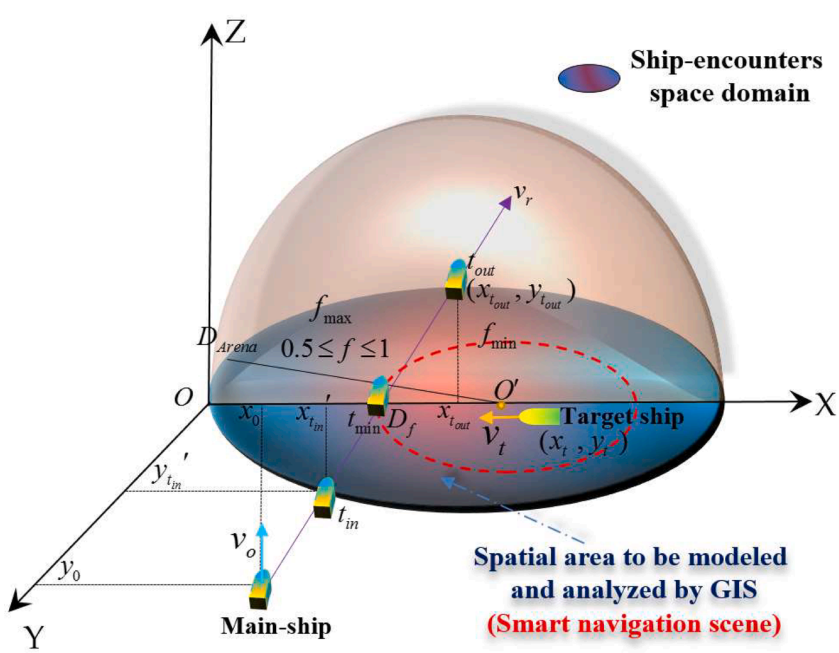

Fig. 8. Spatial computation vector for determining the danger parameters of the ship-encounter space domain in an intelligent navigation scenario. The blue area indicates the spatial area to be modeled and analyzed, while the area encircled by the red dotted line indicates the spatial area formed by two ships at peak danger.

semimajor and semiminor axes can be expressed as $\Delta a = \Delta a_1 + \Delta a_2 =$ 5L and $\Delta b = \Delta b_1 + \Delta b_2 = 2.5$L, respectively, as defined in Fig. 7.

3.2. Analysis of danger in the ship-encounter space domain

The CRI of ships, which is a quantitative expression of the probability of collision during navigation, is a vague concept. To further measure the spatial distribution of the CRI, we propose a collision risk identification parameter based on the spatial calculation of dangerous waters (the minimum scaling factor of dangerous waters) and the collision risk calculation method proposed by Szlapczynski and Szlapczynska [61]. The minimum scaling factor of the ship-encounter space domain is the minimum value of the scaling factor when the main ship and target ship reach the DCPA while maintaining their current speed and course. The specific formula for the minimum scaling factor is as follows:

$$f_{\min} = \frac{D_f}{D_{Arena}}, \tag{1}$$

where D_f represents the DCPA and D_{Arena} indicates where the center of the ship area reaches the distance of the spatial boundary in dangerous waters. $t_{in}$and t_{out} represent the time remaining for the ship to enter and leave the ship-encounter space domain of the target ship, respectively, while $t_{\min}$ is the time required by the ship to reach the minimum encounter point relative to its ship-encounter space domain (the specific meaning of this variable is illustrated in Fig. 8). The determination of this time is affected by the shape of the ship-encounter space domain, the relative position and angle of the two ships, and the relative course and speed of the two ships. Based on the construction of the ship-encounter space domain, $f_{\min}$, t_{in}, and t_{out} are calculated. First, the semimajor and semiminor axes of the ship-encounter space domain are given as $a_{\text{Arena}} = 20$L and $b_{\text{Arena}} = 10$L, respectively. X_e and Y_e represent the relative positions of the center of the offset target ship, as expressed in Eqs. (4) and (5). Further, a_{Domain} and b_{Domain} represent the semimajor and semiminor axes of the ship-encounter space domain, respectively, while C_{t} denotes the heading of the target ship.

Suppose that Δa and Δb are the offsets of the center of the ship-encounter space domain relative to the position of the ship. Then,

$$\Delta a = a_{\text{Domain}}\cos C_{\text{t}} + b_{\text{Domain}}\sin C_{\text{t}}, \tag{2}$$

$$\Delta b = a_{\text{Domain}}\sin C_{\text{t}} - b_{\text{Domain}}\cos C_{\text{t}}. \tag{3}$$

Considering the intruder factor of the ship-encounter space domain, the center offset at scale f needs to be multiplied by the intruder factor of the ship-encounter space domain; thus, the relative position of the center of the ship-encounter space domain of the target ship can be expressed as follows:

$$X_e = x_{\text{r}} + \Delta a * f, \tag{4}$$

$$Y_e = y_{\text{r}} + \Delta \text{b} * f. \tag{5}$$

Considering the relative motion of the two ships, the position of the ship-encounter space domain of the target ship changes with time, and the amount of change is related to the relative speed of the two ships. Thus, the relative position of the center of the ship-encounter space domain of the target ship can be expressed as follows:

$$X_e(t) = x_{\text{r}} + \Delta a * f + v_{\text{r}} t\cos\varphi_{r\_d}, \tag{6}$$

$$Y_e(t) = y_{\text{r}} + \Delta \text{b} * f + v_{\text{r}} t\sin\varphi_{r\_d}, \tag{7}$$

where t is the time variable. Because the calculation of the collision risk parameter based on the ship-encounter space domain considers the target ship as the reference, when the target ship is stationary, the direction of the relative speed of the two ships can be expressed as follows:

$$\varphi_{\text{r\_d}} = \arctan\frac{v_{\text{rx}}}{v_{\text{ry}}} + \sigma, \sigma = \begin{cases} 0 & v_{\text{oy}} - v_{\text{ty}} \geq 0, v_{\text{ox}} - v_{\text{tx}} < 0 \\ \pi/2 & v_{\text{oy}} - v_{\text{ty}} \geq 0, v_{\text{oy}} - v_{\text{ty}} \geq 0 \\ \pi & v_{\text{oy}} - v_{\text{ty}} < 0 \end{cases} \tag{8}$$

Furthermore, the equation for the ellipse representing the region where the target ship encounters danger is expressed as follows:

$$f(t) = \sqrt{\frac{(X_e(t)\cos\alpha + Y_e(t)\sin\alpha)^2}{a^2_{\text{Arena}}} + \frac{(X_e(t)\sin\alpha - Y_e(t)\cos\alpha)^2}{b^2_{\text{Arena}}}}, \tag{9}$$

where $X_e(t)$ and $Y_e(t)$ represent the relative coordinates of the two ships considering the center offset of the ship-encounter space domain with the relative speed of the two ships and α represents the course of the target ship. Based on this equation, the maximum intrusion degree, $f_{\min}$, of the minimum encounter space and the remaining time, $t_{\min}$, to reach the edge of the minimum encounter space can be obtained. To calculate the ship-encounter space domain, *f(t)* is set to 1, and t is determined when the main ship intersects with the target ship. Thus, the remaining time, t_{in} and t_{out}, can be calculated. Fig. 8 illustrates the danger parameters for the ship-encounter space domain to compute the vector graphics.

The distribution of collision risks in the dynamic spatial–temporal domain of ship encounters varies nonlinearly. Based on the above calculation method, the scaling factor $f_{\min}$ of the minimum ship-encounter space domain is obtained first, followed by t_{in} and t_{out}. It represents the degree of the future danger that the two ships will encounter. This supports the following step of revealing the changing spatial hazard trends and characteristic laws in the dynamic spatial–temporal domain of the encounter. The space collision risk is calculated according to the minimum scaling factor, $f_{\min}$, of the target ship, and the collision risk of the two ships can be calculated using Eq. (10).

$$u_s = \begin{cases} 1 & f_{\min} \in [0, 0.5) \\ (2 - 2f_{\min})^{3.03\lambda} & f_{\min} \in [0.5, 1) \end{cases}. \tag{10}$$

When $f_{\min}$ is greater than 1, there is no danger. The temporal risk, u_t, of collision between two ships based on the ship-encounter space domain can be specified by $t_{\min}$, which is expressed by Eq. (11). This equation is inspired by the time collision risk formula based on the TCPA. TCPA is a classic collision avoidance parameter, and most ship pilots still use DCPA/TCPA to guide ship collision avoidance. The time risk between two ships in the ship-encounter space domain can be obtained using Eqs. (11)–(13) and is strongly correlated with the time to reach the closest encounter point in the $t_{\min}$ and $f_{\min}$ of the minimum ship-encounter space domain. When $t_{\min} < t_1$, the danger is at its maximum from the time factor; otherwise, it is at its minimum. When $t_1 < t_{\min} < t_2$, the u_t of collision has a strong correlation with t_1 and t_2.

In Eq. (12), t_1 represents the time of invasion of the target ship. When $f_{\min} \geq 0.5$, the ship does not invade the ship-encounter space domain; thus, $t_1 = 0$. When $f_{\min} < 0.5$, the ship invades the target-ship-encounter space domain and produces a large CRI, and the time it takes for the ship to travel from the boundary of the ship-encounter space domain to the DCPA is expressed using Eq. (12), where R denotes the semimajor axis of the ship-encounter space domain and 0.5R represents the distance between the boundary of the ship domain and the center of the ellipse. Further, $f_{\min}$R represents the distance between the DCPA and the center of the ellipse and t_2 denotes the time when the main ship becomes aware of the target ship (which is calculated using Eq. (13)). The method and principle of calculating the collision risk based on the ship-encounter space domain are described as follows. The spatial–temporal danger results can help reveal the nonlinear spatial characteristics and distribution patterns of ship-encounter danger. This algorithm has passed several sea voyage tests and obtained China CNAS authoritative certification, which guarantees the validity and feasibility of the algorithm results.

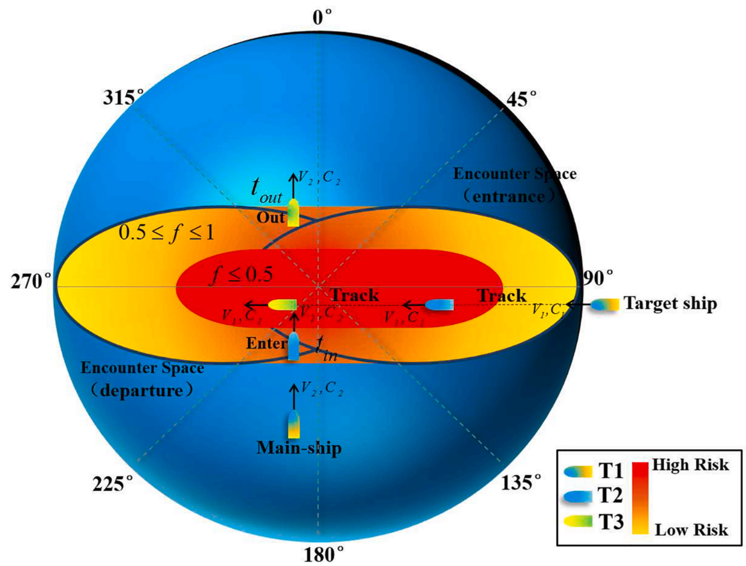

Fig. 9. Schematic of the principle of the ship-encounter space domain based on encountered danger.

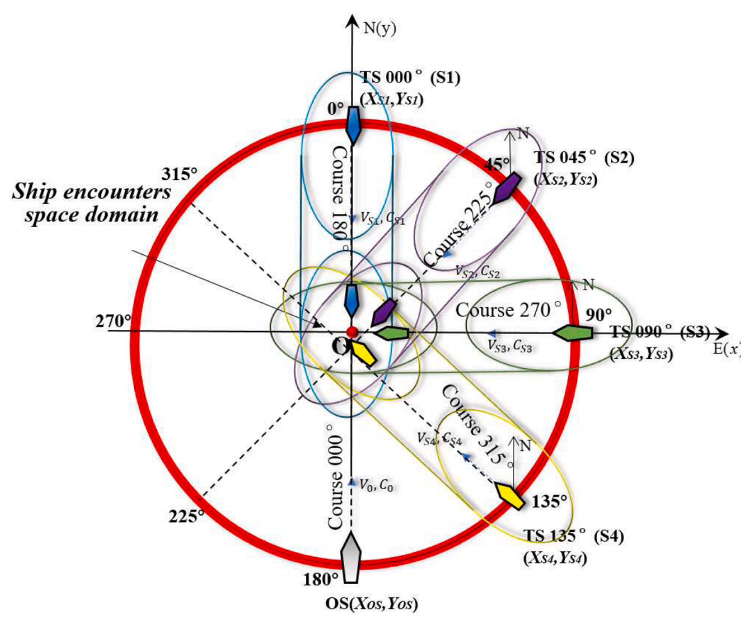

Fig. 10. Schematic of the ship-encounter space domain based on multiship-encounter danger.

$$u_t = (t_2 - t_{\min}) \Big/ (t_2 - t_1)^{3.03\lambda} \quad t_{\min} \in [t_1, t_2] \tag{11}$$

$$t_1 = \begin{cases} 0 & f_{\min} \ge 0.5 \\ \sqrt{(0.5\text{R})^2 - (f_{\min}\text{R})^2} * \dfrac{1}{v_r} & 0 \le f_{\min} < 0.5 \end{cases} \tag{12}$$

$$t_2 = \sqrt{6^2 - \text{R}^2 f_{\min}^2} \Big/ v_r \tag{13}$$

3.3. Spatial modeling and analysis of the ship-encounter space domain

3.3.1. Construction of the multiship-encounter space domain based on encounter danger

We established a multiship-encounter space domain by combining the single-ship-encounter space domain presented in Section 3.1 with the parameters related to multiship encounters and collision risk. Subsequently, we performed spatial modeling and analysis to determine the nonlinear spatial distribution, which revealed the ship-encounter danger within the ship-encounter space domain at a specific time and location. The spatial scope of the ship-encounter space domain model is based on the time when the target-ship-encounter space domain enters the ship-encounter space domain, and the location where the ship encounters danger represents an urgent situation for the pilot while sailing. This includes dangerous waters, where a safe distance must be maintained from the target ship. The time range is constructed using t_{in} (the moment the ship invades the encounters space domain of the target ship) and t_{out} (the moment the ship leaves the encounters space domain of the target ship). Figs. 9 and 10 illustrate the construction principle of the ship-encounter space domain based on the encounter danger and multiship-encounter danger, respectively.

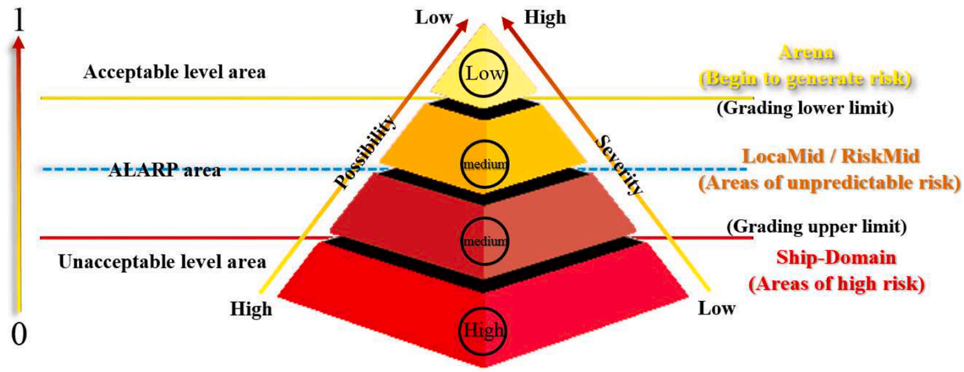

Fig. 11. Classification and construction of the ship-encounter space domain based on the ALARP criterion.

3.3.2. Spatial modeling and analysis of the ship-encounter space domain

3.3.2.1. GIS spatial modeling principle. We performed spatial modeling using GIS spatial analysis methods and advanced mathematical functions to solve complex spatial analysis problems, such as precise extraction and quantification of the complex spatial characteristics and distribution patterns of dynamic and static targets for various time series. The spatial modeling analysis of latent trend features in the space domain was achieved from the perspective of multiple spatial–temporal sequences and navigation states, thereby improving the analysis and GIS-based presentation of information regarding spatial distribution differences and nonlinear spatial trends of ships in danger [63]. Spatial modeling can be based on vector data or raster spatial data [64]. To obtain vector information, object, and field models in the spatial information model were employed for spatial modeling. The spatial modeling method represents spatial entities as mathematical functions, and the modeling results of vector data include the definition and value domains. The definition domain represents the size of the space occupied, whereas the value domain comprises a collection of spatial models. For spatial modeling of spatial raster information, the spatial modeling method performs modeling based on information such as spatial coverage and spatial unit attributes. To further reveal the potential nonlinear spatial characteristics and distribution patterns of the ship-encounter space domain, Section 3.3.2.2 combines vector and raster modeling to construct a GIS spatial modeling and analysis method based on the ship-encounter space domain.

3.3.2.2. Modeling and analysis methods based on the space domain of ship encounters. Spatial modeling and analysis of the time and space characteristics of ship-encounter dangers are major challenges. Spatial modeling employs GIS spatial analysis methods and the corresponding mathematical models to abstract and simplify complex ship-encounter hazards determined via spatial information data and phenomena as well as to quantitatively express the characteristics and laws of spatial processes (ship-encounter processes) [65,66]. Spatial differences occur when a ship encounters danger in each time and space state, and the distribution of hazards in the ship-encounter space domain exhibits nonlinear spatial characteristics and distribution patterns. Extracting these encounter features can considerably improve the spatial analysis of ship-encounter dangers by determining the navigation safety conditions in different ship-encounter spaces and reducing the complexity and uncertainty of the navigation process. Moreover, it can provide ship drivers with accurate and comprehensive ship navigation safety information in real time. The proposed method for modeling the ship-encounter space domain is used to calculate the collision risk of the spatial feature points and to further extract the spatial distribution characteristics of the collision risk in the ship-encounter space domain.

After constructing the ship-encounter space domain, it is necessary to further analyze its risk change trend. The results of encounter risks in different spatial locations may vary. To obtain the spatial distribution of the collision risks in the ship-encounter space domain, key points with the known ship-encounter danger value must first be determined. To improve the accuracy of modeling key points in the ship-encounter space domain, we introduce the as low as reasonably practicable (ALARP) principle to classify the inherent risks in the ship-encounter space domain. ALARP is a risk judgment principle widely adopted for determining the acceptable level of risk in international risk assessment practices. The ALARP framework classifies risks into impermissible risk levels, major permissible risk levels, and risk levels in the ALARP area by establishing two risk demarcation lines. The impermissible risk level indicates that the risk and probability of unacceptable consequences are high, whereas the major permissible risk level indicates that the risk level is low. The ALARP area comprises risk levels between the impermissible risk level and the major permissible risk level.

Therefore, we classified the risk of the ship-encounter space domain according to the ALARP principles. The spatial risk distribution of the constructed ship-encounter space domain conforms to the rules of the ALARP criterion framework for risk classification, classified from low risk to high risk. In the ALARP criterion framework, the impermissible risk level corresponds to the encounter-risk level of the innermost space (ship domain) in the ship-encounter space domain, signifying a relatively high level of risk, where a collision is likely to occur if no collision avoidance action is taken. The ALARP area comprises high- and low-risk levels, where the risk level is moderate. The major permissible risk levels in the ALARP framework correspond to the areas where the ship-encounter space domain begins to exhibit encounter risks. At this time, the risk is at a low level. When a ship encounters danger in the ALARP area, its distribution pattern conforms to the mathematical function of systemic risk. Fig. 11 presents the classification of the ship-encounter space domain based on the ALARP criterion. The method proposed in this study establishes the model feature points of the spatial model of the ship-encounter space domain according to the encounter-risk classification results based on the ALARP criterion framework. This approach enhances the accuracy of spatial modeling and analysis in the ship-encounter space domain. The classification is based on the spatial information platform combined with C# and GIS components, resulting in the expression of the ship-encounter space domain as line elements using elliptical and rectangular boundary vector elements and connecting two semielliptical rectangular boundaries. The obtained center of the ship-encounter space domain and scaling factor are used as risk values at the boundary position. The line elements of the spatial model include the collision risk maximum line element constructed by the boundary of the ship-encounter space domain ($f = 1, u = 0$) and the collision risk zero-value line element constructed by the boundary of the ship-encounter space domain ($f = 0.5, u = 1$). Furthermore, two median lines are added, including the median line of the collision risk ($f = 0.75$, $u = 0.122$) of ships in dangerous waters. To improve the effectiveness and accuracy of spatial modeling, the line elements are converted into

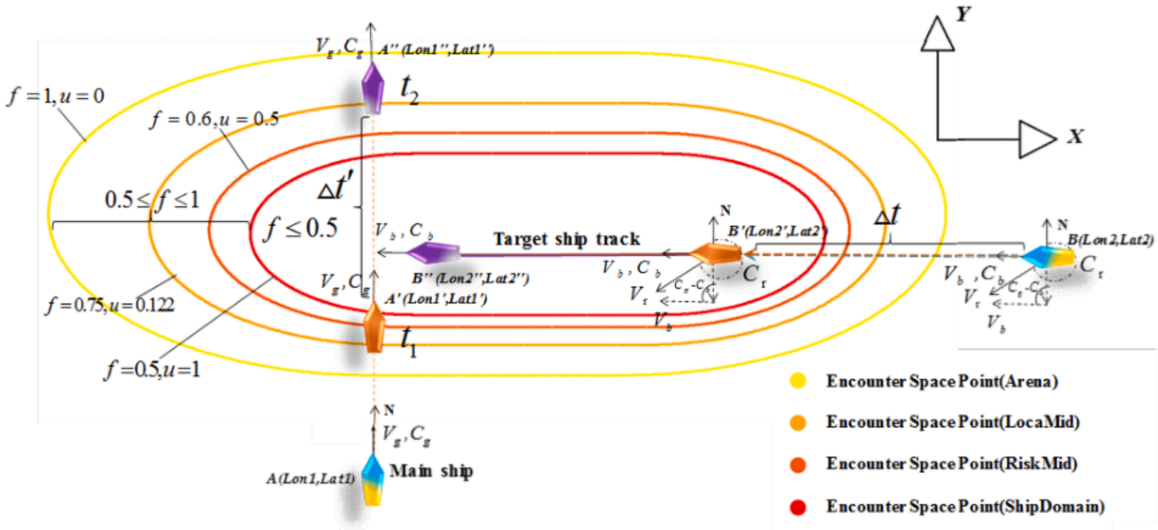

Fig. 12. Schematic of the construction principle of the model feature points in the ship-encounter space domain.

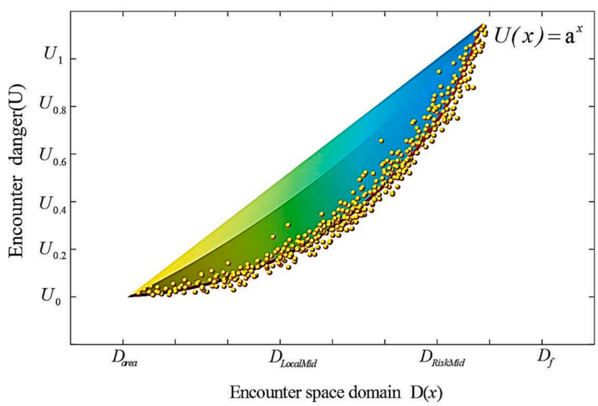

Fig. 13. Mathematical distribution curve of the model feature points in the ship-encounter space domain. The yellow feature points represent random control points in the ship-encounter space domain.

point elements, which serve as the basic spatial units for modeling and analysis of danger in the ship-encounter space domain. Each half of the ellipse comprises 400 model feature points, thereby improving the accuracy of the spatial modeling results. Fig. 12 presents the construction principle of the model feature points in the spatial model of the ship-encounter space domain.

Based on the model feature points of the constructed spatial model of the ship-encounter space domain and the calculation results of the degree of collision risk, we used a spatial information platform to analyze the potential nonlinear spatial feature differences and laws of the ship-encounter space domain in greater detail. To achieve this, we first explored the mathematical distribution pattern of the key points (eigenvalues of the ship-encounter space domain) from the perspective of mathematical functions based on the spatial model of the ship-encounter space domain and the model feature points. Fig. 13 presents the mathematical distribution of the modeled points in the ship-encounter space domain, which was obtained according to the spatial distance distribution of random points. The figure presents the overall change in the exponential function from the boundary to the center of the ship-encounter space domain. The mathematical curve of the model feature points, which is mainly based on power coefficients, improves the accuracy of the spatial modeling of the ship-encounter space domain.

Next, we achieved the interactive spatial calculation and analysis of the original values (eigenvalues of the ship-encounter space domain) and the derived data of all sets of positions in the ship-encounter space domain based on the spatial sequence of the ship-encounter space domain, collision risk identification parameters, and relative spatial position distribution of the ships. Consequently, we were able to determine the spatial distribution pattern and spatial trends of the encounter hazards in the set of all locations in the ship-encounter space domain in the continuous spatial–temporal state.

In summary, using the proposed GIS spatial modeling and analysis method, the spatial domain of dangerous encounters under multi-temporal and multiangle conditions can be modeled and analyzed and in-depth analysis and perception of the changing trends and distribution patterns of the ship-encounter space domain for a multitemporal sequence and nonlinear space can be achieved. Additionally, the spatial ambiguity of the collision risk can be clarified.

Furthermore, in the spatial modeling process, we first analyzed the hazard value of the encounter space model feature points and then constructed a variogram and covariance function to calculate the hazard distribution of other encounter space regions. The spatial properties of any point $u(x,y)$ are assumed to be uniform, signifying that any point in the space has the same mathematical expectation, c, and variance, σ^2. Furthermore, the value at $u(x,y)$ in the space is considered as the sum of the average values of the area and the random deviation, $R(x,y)$, at that point, which is expressed as follows:

$$E[u(x,y)] = E[z] = c, \tag{14}$$

$$Var[u(x,y)] = \sigma^2, \tag{15}$$

$$u(x,y) = E[u(x,y)] + R(x,y) = c + R(x,y), \tag{16}$$

where $R(x,y)$ represents the deviation of point u. The variance is assumed to be constant. We used empirical semivariograms, including spherical, exponential, Gaussian, linear, and trigonometric function types. The result of the spatial modeling of the ship-encounter space domain was obtained using the exponential semivariogram method as follows:

$$\widehat{\mu}(s_0) = \sum_{i=1}^{n} \lambda_i \mu_i(s_i) \quad \widehat{\mu} \in a^i, \tag{17}$$

$$\widehat{\mu}_0 - E[u] = \sum_{i=1}^{n} \lambda_i \mu_i(s_i - E[u]). \tag{18}$$

Parameterλ_i is dependent on the fitting model of the distance between the key spatial point and the estimated point of the ship-

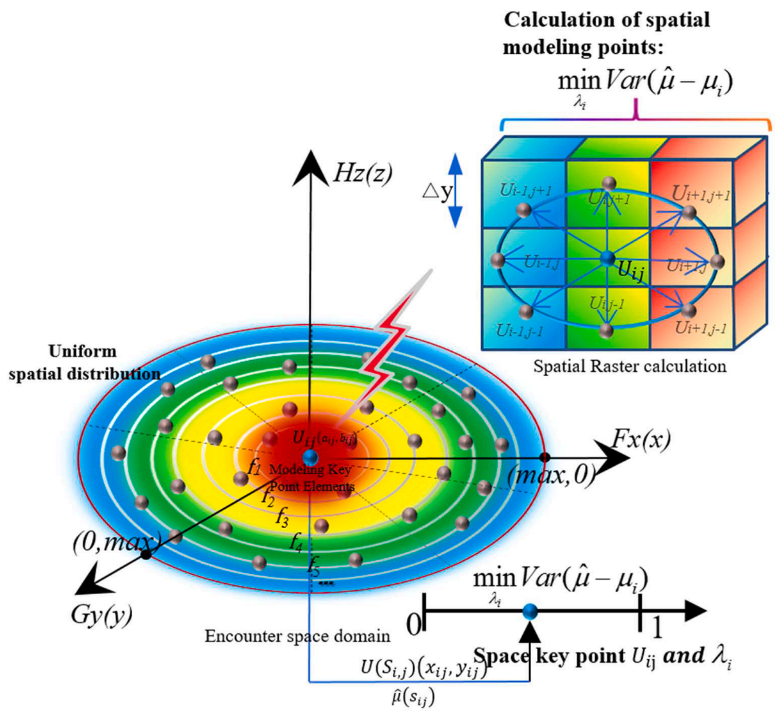

Fig. 14. Schematic of the spatial modeling method for the ship-encounter space domain based on the GIS.

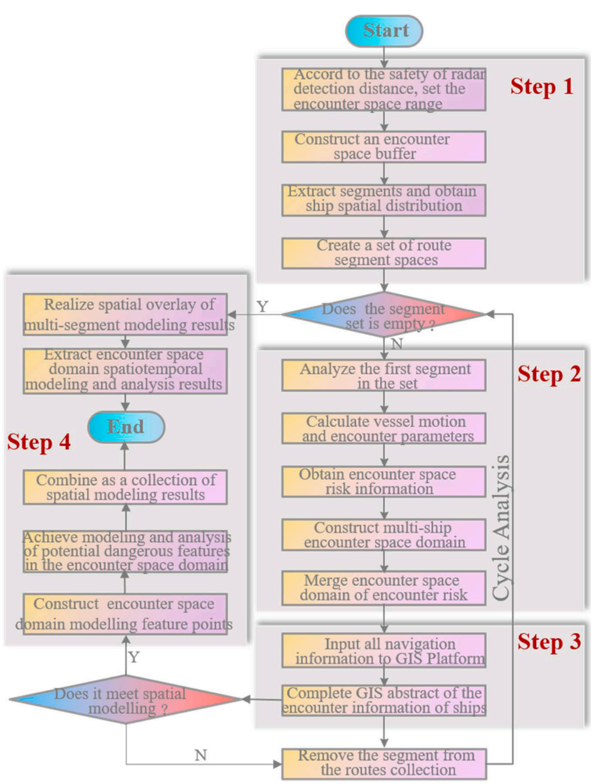

Fig. 15. Basic steps of modeling and analysis of the ship-encounter space domain in multisegment navigation scenarios.

encounter space domain and the spatial relationship between the key spatial points around the estimated point. Using the set of optimal coefficients with the smallest difference between the estimated value of each point and the true value, the optimization goal of λ_i is expressed as follows:

$$\min_{\lambda_i} Var(\widehat{\mu} - \mu_i), \quad (19)$$

where the optimal set of λ_i is used in the spatial modeling of the ship-encounter space domain.

In Fig. 14, the red-to-blue intervals represent the influence of the center point (spatial modeling feature point) on the surrounding spatial area, with different colors indicating different magnitudes of influence. The modeling principle of the ship-encounter space domain is illustrated using the blue ellipse presented in the right part of Fig. 14 as an example. The ellipse is surrounded by eight uniformly distributed point elements with the same mathematical expectations and variances. This modeling process is implemented on a spatial information platform, mainly using the spatial modeling method based on raster objects. The blue ellipse represents one of the space units in the sea area where a ship may encounter danger. By taking the center position of the spatial model of the dangerous sea area as the modeling key point $U_{i,j}(u_{ij}, u_{ij})$, other modeling points in the neighborhood space, such as $U_{i-1,j+1}$, $U_{i,j+1}$, and $U_{i+1,j+1}$, are calculated. The modeling results of all continuous spatial distributions in the ship-encounter space domain can be obtained by repeating these calculation steps. These spatial modeling results can be used to further discover and explain the spatial distribution and changes in the hazard degree in the ship-encounter space domain. Based on the construction principles of the modeling and analysis method for the entire ship-encounter space domain, Fig. 15 illustrates the basic steps of the method for the ship-encounter space domain in multisegment navigation scenarios. This facilitates the development of case simulation studies of the proposed method.

4. Applications of the proposed method and discussion

In Section 3, the spatial modeling and analysis method for the ship-encounter space domain was described in detail. To further illustrate the accuracy and effectiveness of the proposed method, we simulated different ship-encounter scenarios. The simulation cases can be divided into two encounter scenarios with navigation hazards: (i) a ship navigation scenario with a turning-point route and (ii) a ship navigation

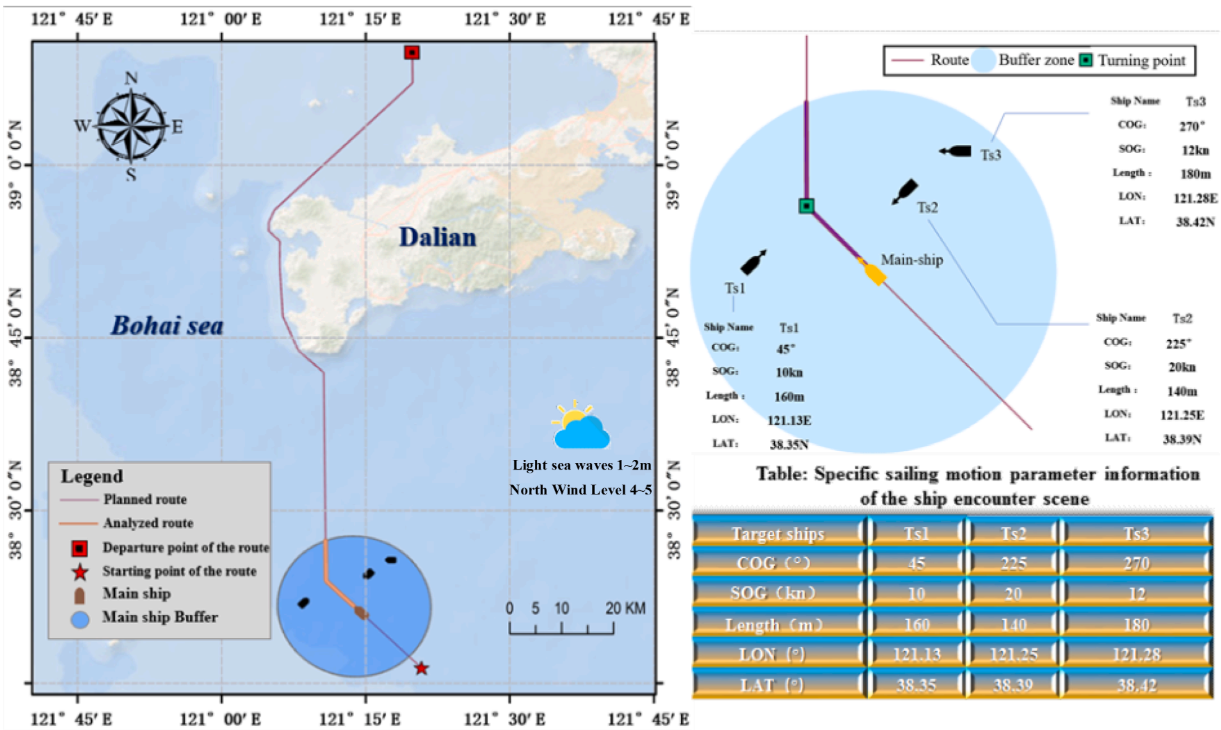

Fig. 16. Ship-encounter scenario and navigation-motion parameter information in the selected part of the real sea area (used as the example simulation scenario to evaluate the applicability of the proposed method).

scenario with a straight-line segment. Analysis of the example scenarios indicates that the proposed method can effectively extract continuous spatial distribution information and spatial–temporal variation trends of potential navigation hazards. Furthermore, we analyzed the reliability of the simulation results of the proposed method, and the results further demonstrate that the proposed method exhibits good accuracy and effectiveness. The key steps in the application of the proposed method include the preprocessing of simulated data, spatial modeling of the ship-encounter space domain, time-series analysis of the modeling results, and analysis and determination of the spatial–temporal heterogeneity of the ship-encounter space domain based on Moran's I index.

This section is divided into four subsections. Section 4.1 presents the simulations of the encounter scenarios with turning points, while Section 4.2 presents the simulations of encounter scenarios with a straight-line segment. Sections 4.1 and 4.2 demonstrate that the proposed method is applicable to straight-line and turning-point scenarios in open water. Section 4.3 compares and verifies the accuracy and reliability of the method. Finally, Section 4.4 discusses the simulation results of the study case, effectiveness of the method, and limitations of the method.

4.1. Simulation of the encounter scenarios with turning points

This subsection is based on the simulation of the ship-encounter scenarios with the turning point to further verify the effectiveness and reliability of the proposed method. First, the detailed information of the application example, including the basic technical parameters of the ship and the information of the navigation waters as well as the preprocessing process of the navigation information, is introduced. Second, the simulation analysis of the method is performed based on a ship-encounter scenario with a turning point, and the continuous spatial distribution information and the spatial–temporal variation trends of potential navigation hazards in this scenario are effectively extracted. The simulation results of the method are deeply analyzed. Finally, the simulation results of the method are analyzed thoroughly. Next, this section describes the related work in detail in the form of Sections 4.1.1 and 4.1.2.

Table 2
Basic technical parameters of the main ship (M/V YU KUN).

Serial number	Ship parameters	Information
01	Length between perpendicular	116 m
02	Molded depth	8.3 m
03	Breadth	18 m
04	Draft design	5.4 m
05	Service speed	15 kn
06	Rudder area	11.8 m^2
07	Rudder height	4.8 m
08	Mean power of the main engine	18,860 kW
09	Ship speed through water (U)	16 kn

4.1.1. Application examples and data preprocessing

We investigated the effectiveness of the proposed method in an encounter scenario with navigational hazards. First, ship simulation data were input into the spatial information platform and spatial position coding and geometric correction were performed in the spatial preprocessing. Considering the coastal waters of Dalian, China, as a case study, the ship navigation information of the real electronic map is provided in Fig. 16.

The turning-point and straight-line-segment sailing scenarios were set up to experimentally verify the effectiveness of the proposed spatial modeling and analysis method for the ship-encounter space domain. At 38.35°N and 121.21°E, the main ship, named M/V YU KUN, with a length of 116 m traveled at a speed of 12 kn and a heading of 315° It encountered open water with good visibility when driving 7036 m away from the waypoint along the planned route. At this time, the course of the ship was changed to 0°, and the main ship encountered three target ships with courses of 45°, 225°, and 270° The three target ships maintained constant direction and speed. Table 2 lists the basic operations and technical parameters of the main ship. Fig. 16 presents the basic information of the real encounter scenario used in this simulation, which is a part of the voyage of a ship in the Bohai Sea area of Dalian, China. The sea was cloudy with good visibility, with northerly winds of

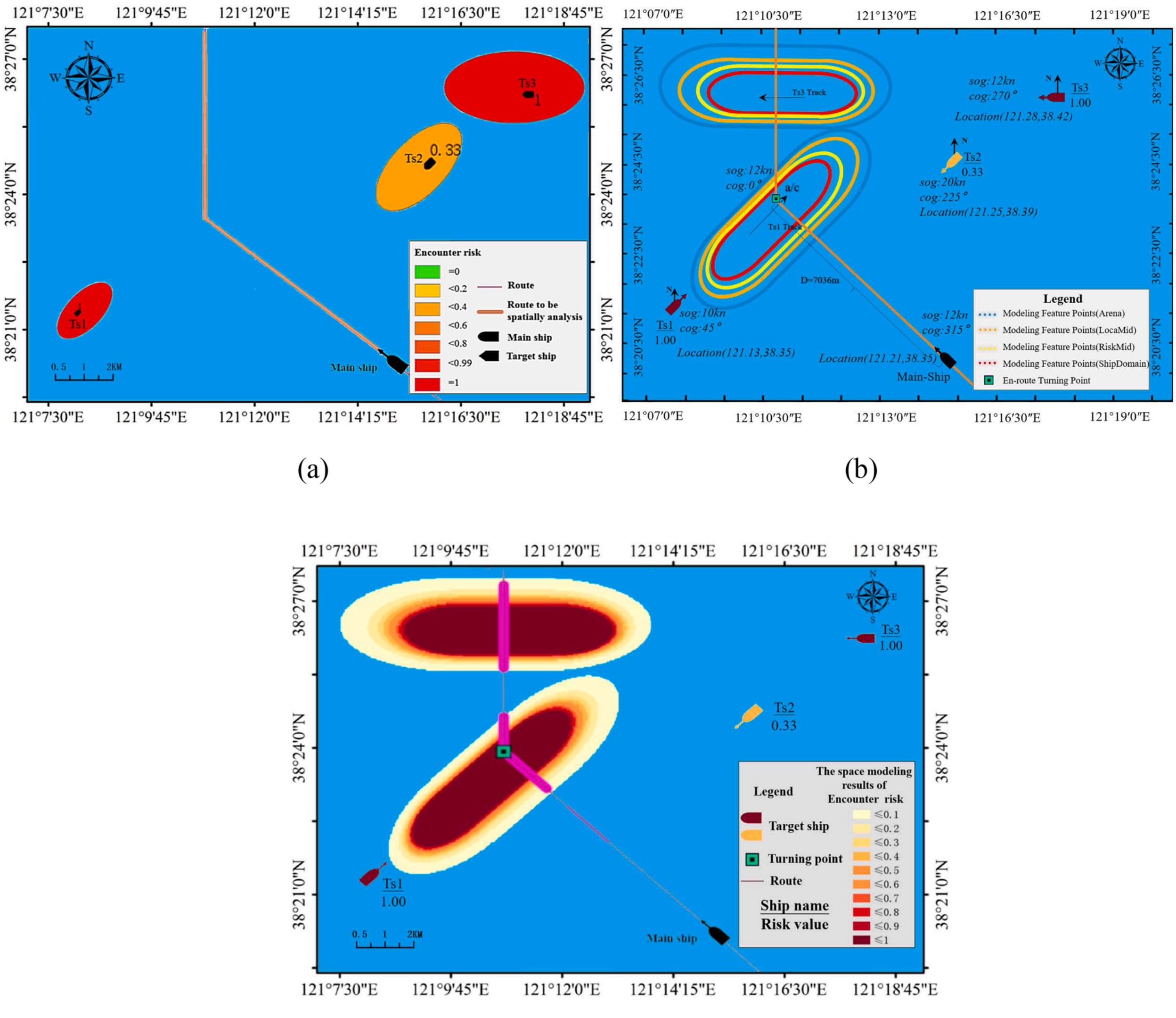

Fig. 17. Spatial computing, modeling, and analysis results of the ship-encounter space domain at a turning point in the spatial information platform: (a) identification and analysis results of the collision risk for target ships in the buffer zone (before turning); (b) encounter space model feature points; (c) spatial modeling results of the ship-encounter space domain.

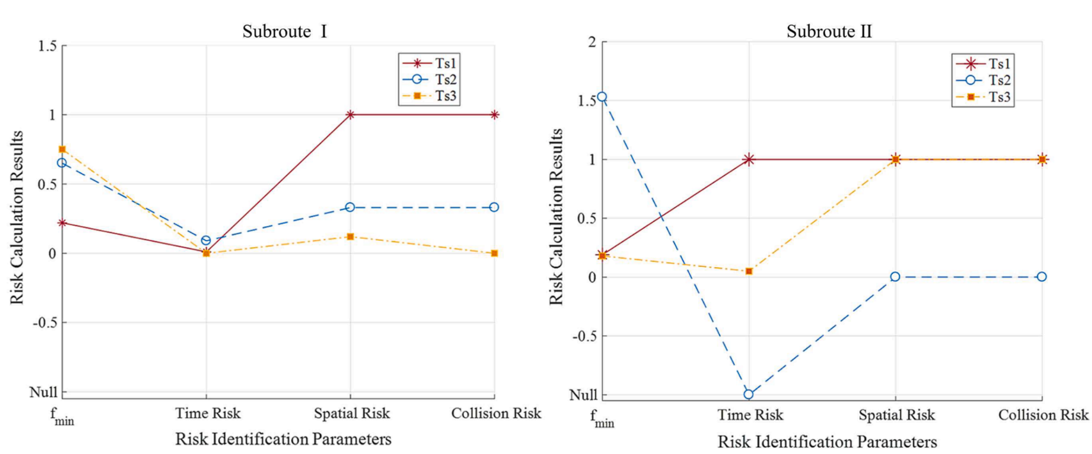

Fig. 18. Calculated collision risk of ships in the ship-encounter space domain: (a) Subroute I and (b).

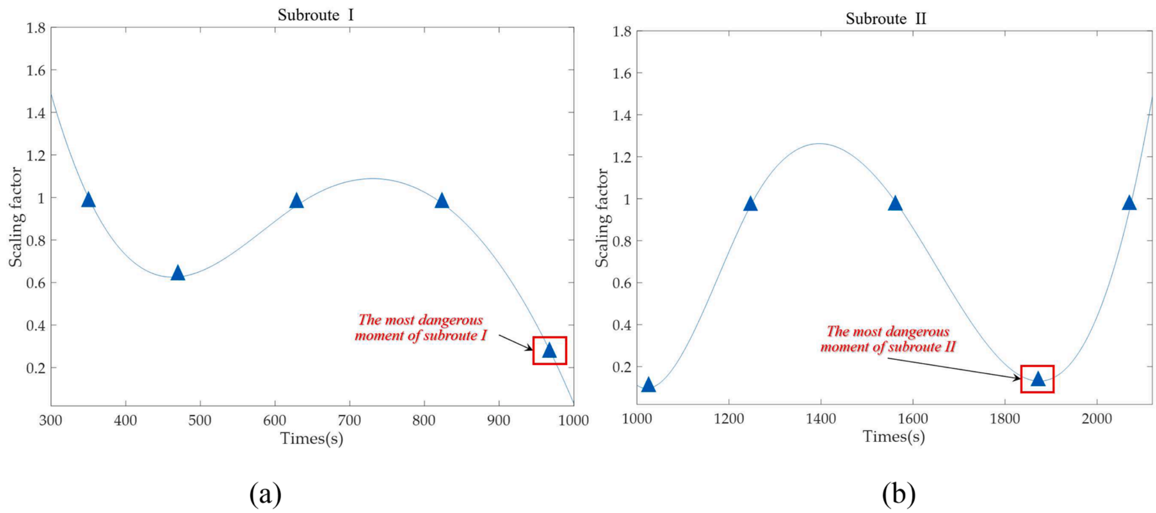

Fig. 19. Time-series information on collision risk in the ship-encounter space domain in routes with a turning point: (a) Subroute I and (b) Subroute II.

magnitude 4–5 and light waves of 1–2 m on the sea surface. The ship encountered target ships (TS1, TS2, and TS3) in open water, and there were no obstacles, such as sunken ships and reefs. The water depth was ~50 m according to the chart. This represents a set of sailing scenarios with turning points. Information regarding the selected sea area and ship navigation space was input into the space information platform, and spatial modeling and analysis of the ship-encounter space domain were performed to extract the spatial distribution and changes in navigational hazards.

4.1.2. Modeling and analysis results of the ship-encounter space domain

The calculation process of spatial modeling and analysis using the ship-encounter space domain involved inputting information regarding the selected water area and ship navigation space into the spatial information platform, followed by extracting the spatial laws and characteristics of the ship-encounter space domain. The point elements included the start and end of the turning point and one waypoint, while the line element included two subroutes divided by the waypoint. Analysis of the navigation time at the first turning point indicated that it took 1140s to reach the next waypoint at the current sailing speed. Based on the collision-hazard identification algorithm in the ship-encounter space domain, the collision-hazard results of the main ship and each target ship in Subroute I was obtained. When the ship sailed to the next subroute, the spatial position of the target ship was determined based on the sailing time. The ship collision risk was evaluated based on the collision risk identification algorithm in dangerous waters, and the collision risks of TS1 and TS3 were identified as 1. The spatial model of the ship-encounter space domain was then constructed according to the collision risk identification parameters and hazard calculation results of TS1 and TS3. According to the spatial order of the ship-encounter space domain, interactive spatial calculations and analyses were conducted on the calculated and derived values for ships encountering danger. Thus, spatial modeling and analysis of the ship-encounter space domain were achieved to obtain the trend and distribution characteristics of potential hazards in the space domain of ship encounters from a multistate spatial–temporal perspective.

Fig. 17 presents the results of the spatial computation, modeling, and analysis of the ship-encounter space domain with a turning point based on the spatial information platform. The results of spatial modeling indicate that TS1 and TS3 are dangerous areas in space, greatly affecting the route of the main ship. In contrast, TS2 has a lower encounter danger of 0.33, which is a safer encounter state than that of the main ship. Fig. 18 presents the calculated collision risk of ships in the ship-encounter space domain, providing a more intuitive representation of

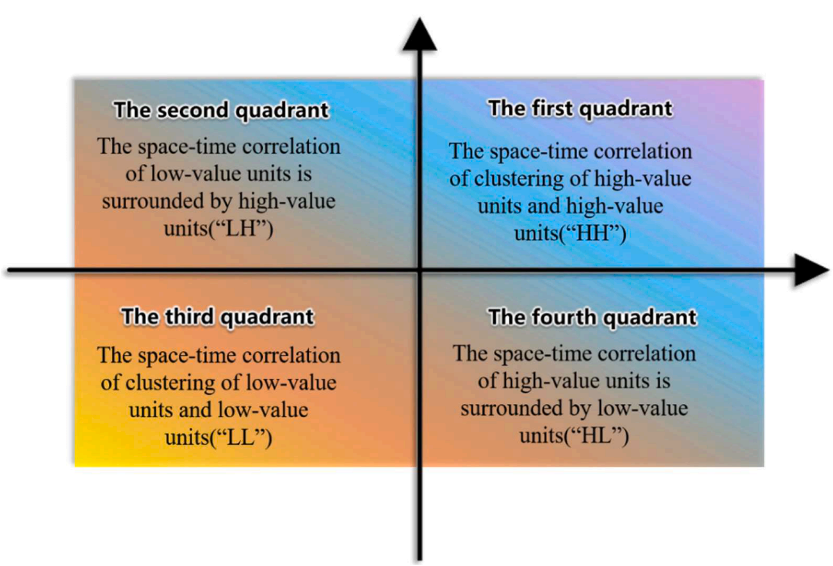

Fig. 20. Four-quadrant representation of the space–time correlation form of units that encounter danger.

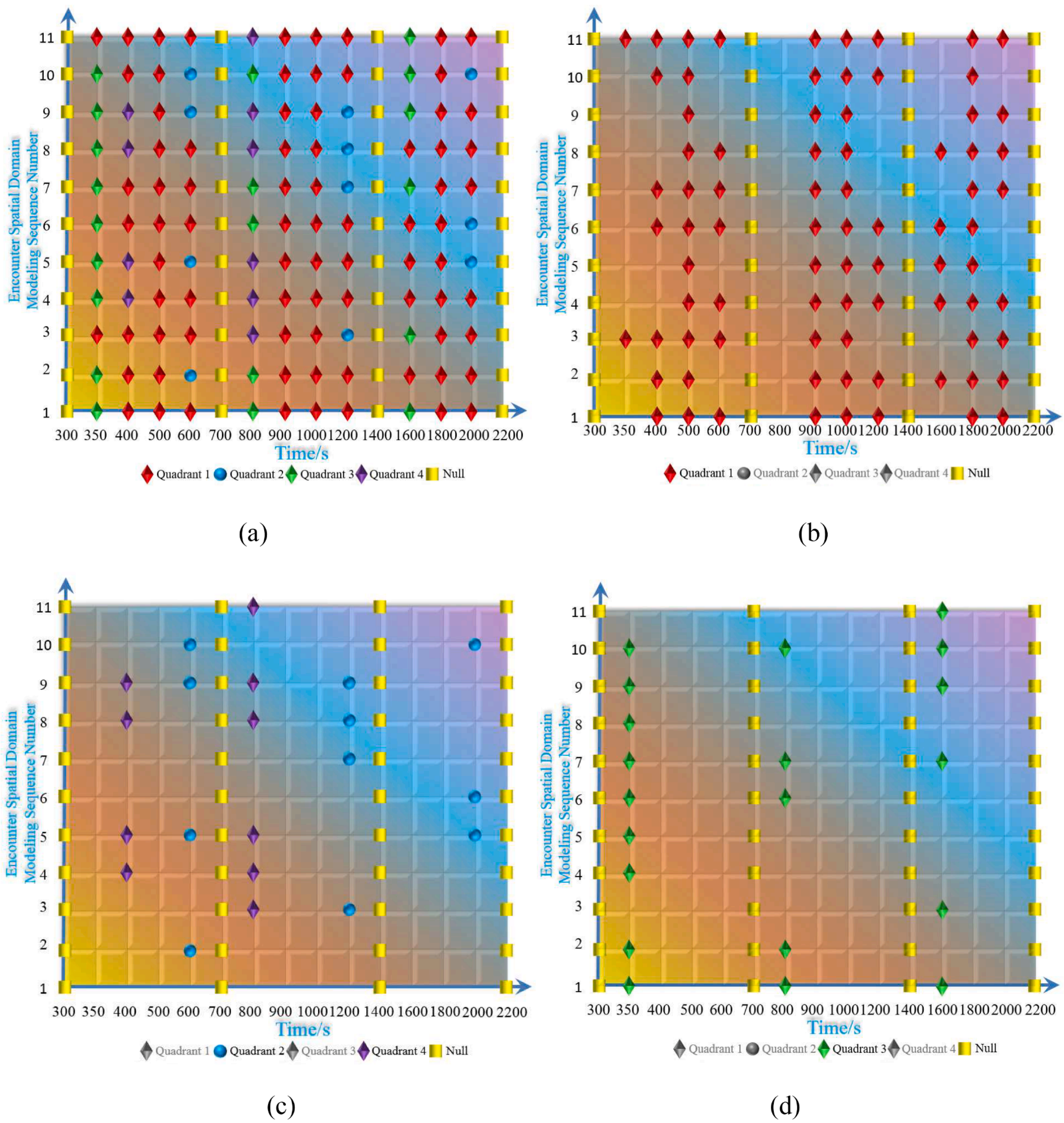

Fig. 21. Spatial and temporal heterogeneity features in the ship-encounter space domain at a turning point based on Moran's I index modeling results: (a) overall spatial–temporal distribution and associated characteristics of the danger value; (b) spatial–temporal distribution state and associated characteristics of the high-danger-value spatial units; (c) spatial–temporal distribution state and associated characteristics of the interconnected spatial units with low and high degrees of danger; (d) spatial–temporal distribution state and associated characteristics of the spatial units with a low degree of danger.

the risk associated with TS1, TS2, and TS3 encountering the main ship. Additionally, the time-series analysis and calculation of the ship-encounter space domain enable the identification of spatial–temporal changes in dangerous waters in Subroutes I and II. Fig. 19 presents the time-series information on dangerous waters in the ship-encounter space domain along these routes. The numerical distributions of Subroutes I and II conform to the polynomial equations

$$y = 2.6 \times 10^{-11} x^4 - 1.5 \times 10^{-7} x^3 + 0.00031 x^2 - 0.28x + 91 \tag{20}$$

and

$$y = 5.8 \times 10^{-11} x^4 - 1.9 \times 10^{-7} x^3 + 0.0002 x^2 - 0.093x + 16, \tag{21}$$

respectively.

To further analyze the overall spatial–temporal heterogeneity and spatial homogeneity of the ship-encounter space domain, Moran's I index was used to analyze the local spatial–temporal distribution of the domain [67]. First, Moran's I index was calculated based on the position number of model feature points in the ship-encounter space domain; then, the distribution feature information and adjacent spatial–temporal object units were obtained. Fig. 20 presents the spatial and temporal distribution characteristics (spatial aggregation, heterogeneity, and correlation) of the ship-encounter space domain based on Moran's I index in four quadrants. Each quadrant represents a different degree of local spatial correlation between adjacent cells in the ship-encounter space domain. The first quadrant represents the space–time correlation form in which the high-danger-value unit is surrounded by the same high-value space. The second quadrant represents the space–time

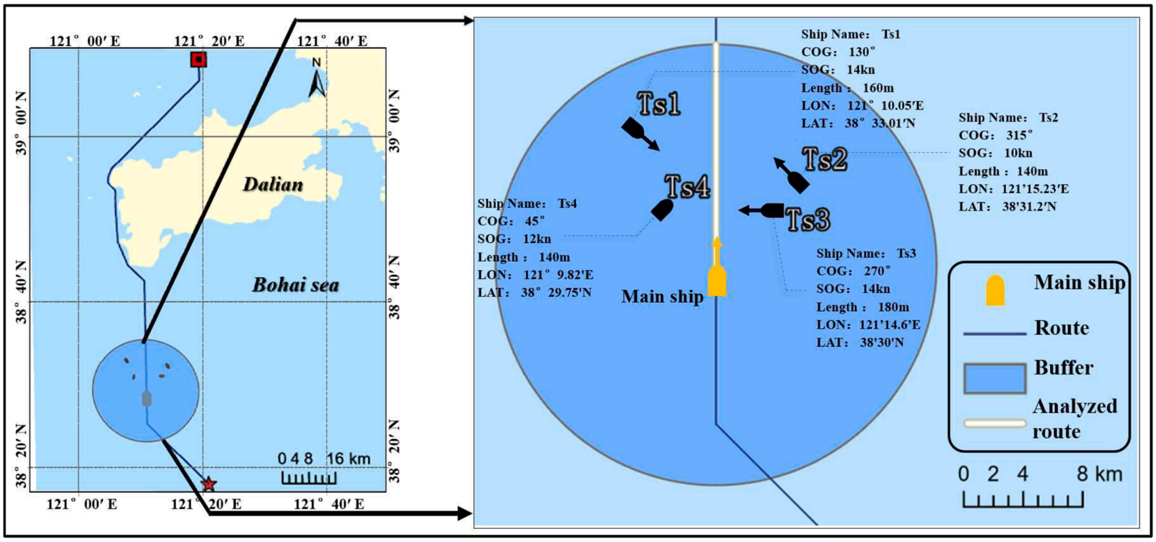

Fig. 22. Encounter scenario and navigation information of ships in the straight-line segment.

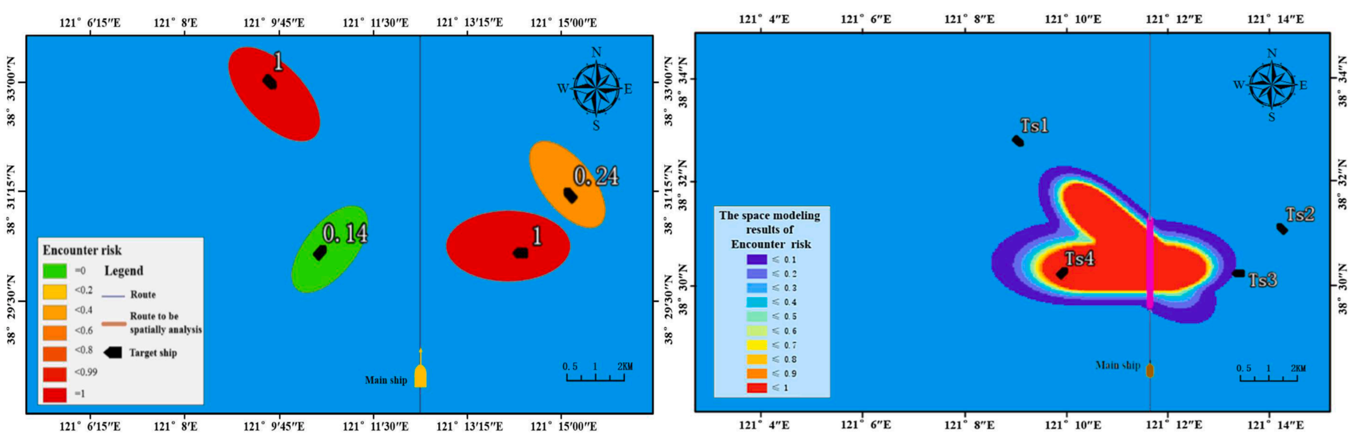

(a) (b)

Fig. 23. Spatial computing, modeling, and analysis results of the ship-encounter space domain in a straight-line segment on the spatial information platform: (a) identification and analysis results of the collision risk of target ships in the buffer zone; (b) spatial modeling results of the ship-encounter space domain.

correlation form in which the low-danger-value unit is surrounded by a high-value space. The third quadrant represents the space–time correlation form in which the low-danger-value unit is surrounded by the same low-value space. The fourth quadrant represents the space–time correlation form in which the high-danger-value unit is surrounded by a low-value space. Fig. 21 provides an intuitive description of the four-quadrant representation of the space–time correlation form of units that encounter danger. The abscissa of the mathematical quadrant in the four-quadrant presentation represents the dynamic time series of ship encounters (ranging from 300 to 2200s), with each time value indicating the cumulative time of ship encounters. The ordinate in the mathematical quadrant represents 11 equidistantly divided waypoint sets (1–11) in the ship-encounter space domain based on the Euclidean distance. For example, 1 signifies the first waypoint in the ship-encounter space domain, while 2 signifies the second waypoint in the ship-encounter space domain. This four-quadrant presentation was used to express the spatial–temporal heterogeneity and spatial homogeneity results of all waypoints (11 in total) in the ship-encounter space domain during the time period from 300 to 2200s. Fig. 21 uses object points of different colors and shapes to reveal the spatial and temporal heterogeneity of the modeling results in the local ship-encounter space domain for the four-quadrant straight-line segment route in an intuitive and detailed manner. It demonstrates that the ship-encounter space domain exhibits spatial–temporal distribution characteristics of high aggregation, strong correlation, and few outliers.

4.2. Simulation of the encounter scenario with a straight-line segment

To verify the accuracy of the proposed method for the ship-encounter space domain, we selected another straight-line-segment scenario from a real sailing route. Fig. 22 displays the encounter scenarios and navigation information of ships in the straight-line segment. The dynamic navigation information of the ship was obtained by analyzing the ship-encounter space domain in the straight-line segment. Using the proposed method, we performed interactive spatial calculation and analysis of the calculated and derived values of the ship-encounter danger based on the value of the ship collision risk parameter. Furthermore, we used the proposed method to perform spatial modeling and analysis of the airspace where the ship encounters occurred and obtained the spatial distribution and change trends of the navigational hazards. Fig. 23 presents the results of the spatial computing, modeling, and analysis of the ship-encounter space domain in a straight-line segment on the

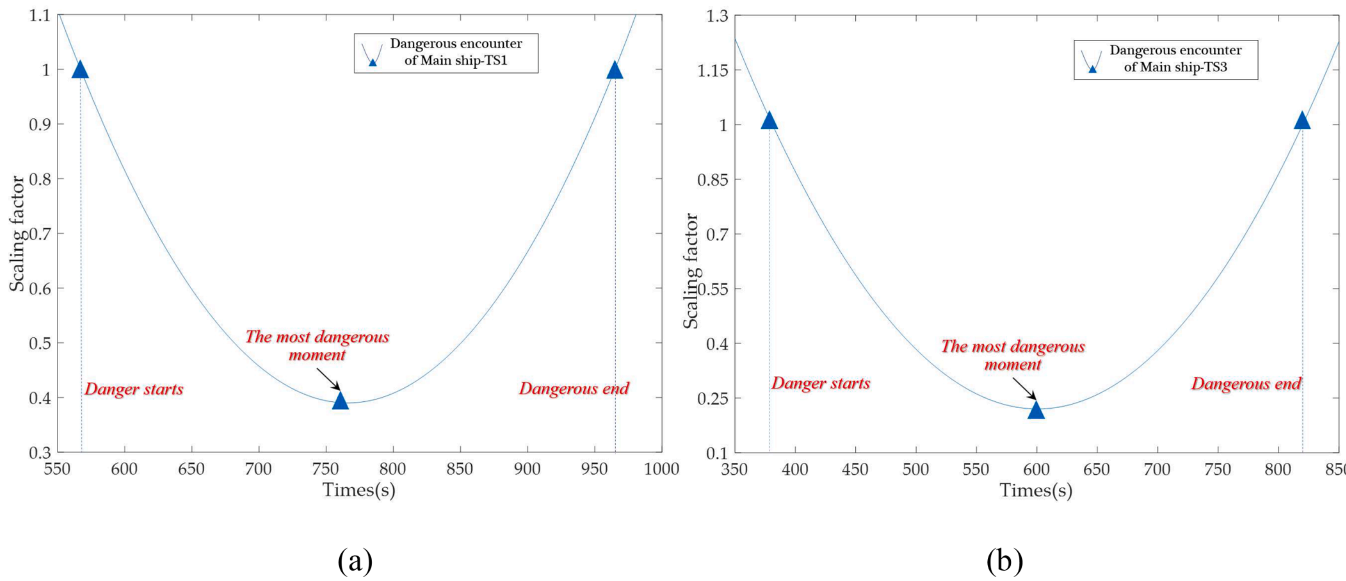

Fig. 24. Time-series analysis results of different target ships in dangerous waters in the route with a straight-line segment: (a) main ship–TS1, (b) main ship–TS3.

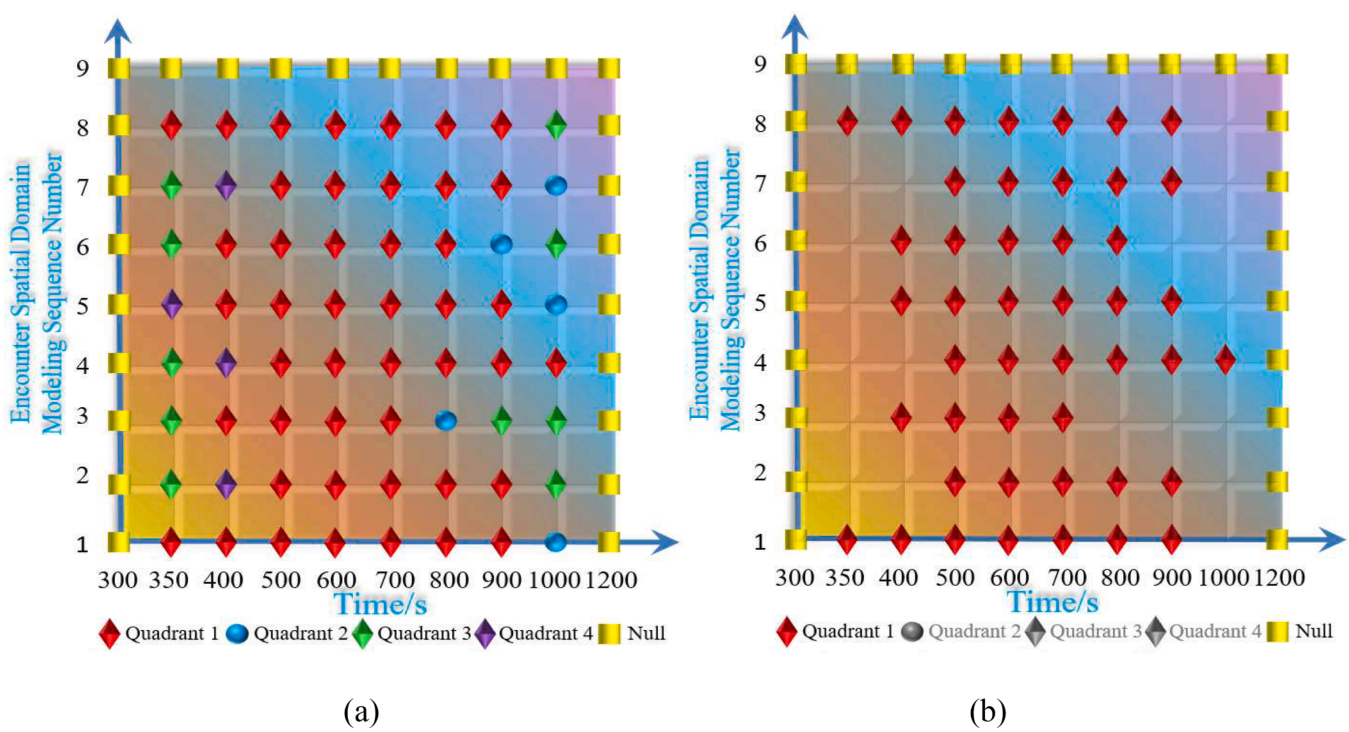

Fig. 25. Spatial and temporal heterogeneity features in the ship-encounter space domain in a straight-line segment based on Moran's I index modeling results: (a) overall spatial–temporal distribution and associated characteristics of the danger value; (b) spatial–temporal distribution and associated characteristics of the high-danger-value spatial units.

spatial information platform. The spatial modeling results revealed that TS1 and TS3 encountered more danger zones in space, which severely affected the navigation of the main ship, while the remaining ships were in a safe encounter state. Fig. 24 presents the detailed time-series analysis results of different target ships in the dangerous waters of this route. The main ship and TS1 form a ship-encounter space domain between 567 and 965 s, with a danger value of 0.39. TS1 and TS3 pose a threat to the navigation of the main ship, and the main ship should take timely action to avoid a collision. The numerical distributions presented in Figs. 24(a) and 24(b) conform to the parabolic functions

$$y = 1.5 \times 10^{-5}x^2 - 0.024x + 9.4 \tag{22}$$

and

$$y = 1.6 \times 10^{-5}x^2 - -0.019x + 6.1, \tag{23}$$

respectively.

Fig. 25 illustrates the spatial and temporal distribution characteristics, including spatial aggregation, heterogeneity, and correlation, obtained from the ship-encounter space domain modeling based on Moran's I index in the four quadrants. The object points, represented by

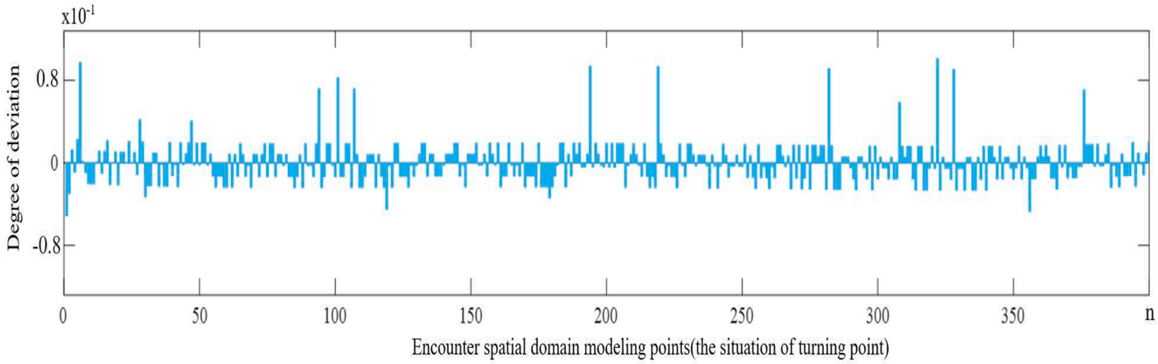

(a)

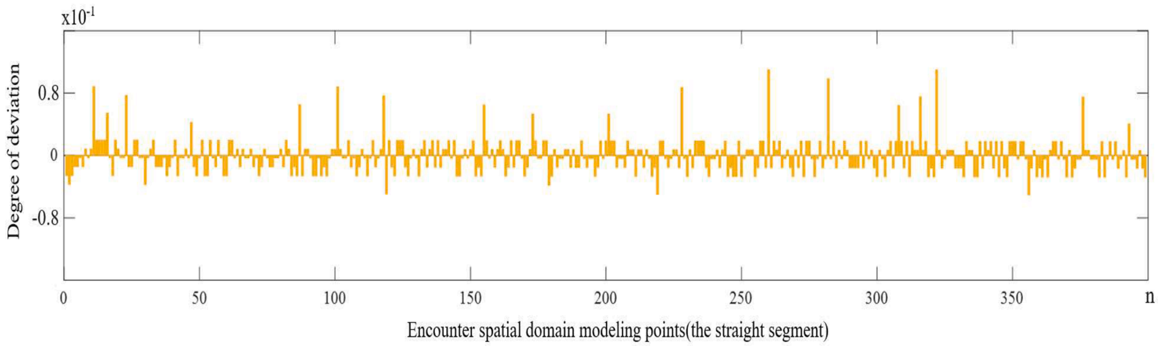

(b)

Fig. 26. Spatial outlier analysis of the modeling results in the ship-encounter space domain: (a) outlier analysis results at a turning point; (b) outlier analysis results in a straight-line segment.

different colors and shapes, indicate the spatial and temporal heterogeneity of the modeling results within the local ship-encounter space domain in the four-quadrant straight-line-segment route. The ship-encounter space domain also exhibits spatial–temporal distribution characteristics of high aggregation, strong correlation, and few outliers.

4.3. Accuracy and reliability verification of the spatial modeling and analysis method

To evaluate the reliability and effectiveness of the proposed method in extracting characteristic information related to the spatial distribution and change characteristics of hazards in a multistate spatial–temporal ship-encounter space domain, we analyzed the spatial outlier degree of the ship-encounter space domain. The spatial outlier analysis method can be used to quickly identify the outliers exceeding a certain confidence interval in the modeling and analyze the results of the encounter-danger space. A lower outlier degree indicates better spatial modeling and analysis, which can more accurately reflect the spatial distribution and changes in the ship-encounter space domain. The larger the outlier, the worse the spatial modeling and analysis results. Fig. 26 displays the results of the spatial outlier analysis. The spatial outlier analysis results of the two encounter scenarios are relatively stable; the maximum outlier is only $\sim 0.8 \times 10^{-1}$, and the overall outlier is 0.3×10^{-1}, which also shows the validity of the simulation results. Additionally, we constructed several evaluation point sets with fixed locations and known collision risks in the ship-encounter space domain based on a spatial modeling algorithm to further evaluate the accuracy of the proposed method. These evaluation point sets were used to assess the accuracy of the spatial modeling results of the ship-encounter space domain. The spatial scaling factors of the ship-encounter space domain at different scales were constructed according to the position of the target ship at t_{in} and t_{out}. The actual endpoint position was then determined from the spatial center of the ship-encounter space domain. Finally, six evaluation points were generated for each scaling factor

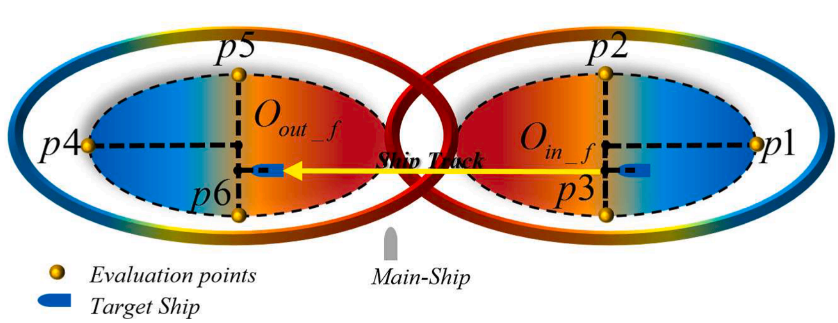

Fig. 27. Construction of the ship-encounter space domain for spatial modeling of the evaluation points.

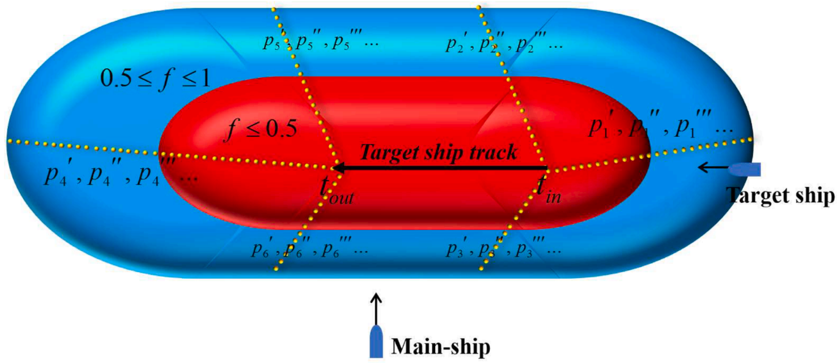

Fig. 28. Construction results of the evaluation point sets in the ship-encounter space domain.

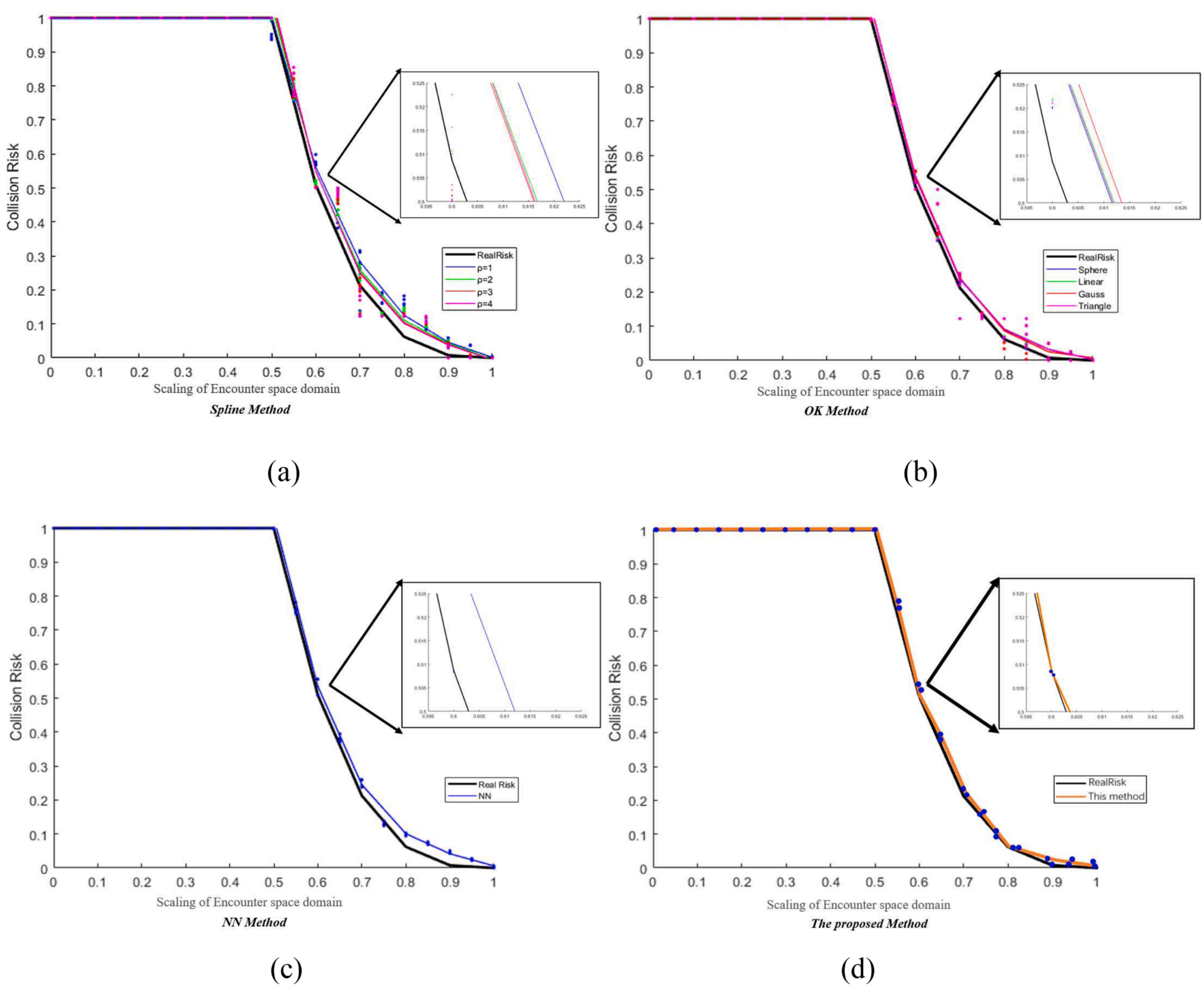

Fig. 29. Comparative analysis of the fitting accuracy of the encounter risk between the proposed method and other modeling methods: (a) spline method; (b) ordinary kriging (OK) method; (c) natural neighbor (NN) method; and (d) proposed method.

level. The spatial collision risk of the evaluation points was calculated using the algorithm described in Section 2.2. Fig. 27 displays the specific technique for generating the error evaluation points.

In Fig. 27, O_{in_f} and O_{out_f} represent the centers of the ellipse for the ship-encounter space domain invasion factor, f, at t_{in} and t_{out}, respectively. The semimajor and semiminor axis offsets relative to the position of the ship are given by $\Delta a_f = f * \Delta a$ and $\Delta b_f = f * \Delta b$, respectively. The position of the center of each field, O_f, relative to Ts can be expressed using Eqs. (36) and (37). Considering the set of space points for the modeling factor in the ship-encounter space domain as the key evaluation point, the construction results of the evaluation point set in the ship-encounter space domain are presented in Fig. 28.

$$O_f(X) = Ts(X) + \Delta a_f \mathrm{Cos}(\alpha) + \Delta b_f \mathrm{Sin}(\alpha), \quad (36)$$

$$O_f(Y) = Ts(Y) + \Delta a_f \mathrm{Sin}(\alpha) - \Delta b_f \mathrm{Cos}(\alpha). \quad (37)$$

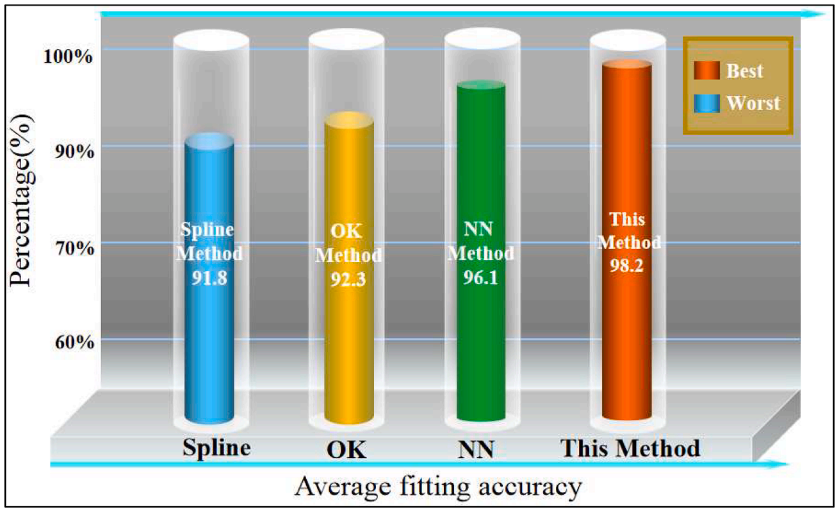

Fig. 30. Fitting accuracy results of the proposed method compared to the other three methods.

The accuracy of the spatial modeling and analysis results was calculated using the established ship-encounter space domain evaluation point sets. First, we used the bilinear and piecewise fitting functions to extract the predicted value of the risk degree of the evaluation point-set space neighborhood unit. Then, we performed piecewise numerical fitting on the encounter-hazard degree of all the location sets in the ship-encounter space domain of each ship to obtain the accuracy of the proposed method and other modeling methods. Fig. 29 compares the results of the proposed method and other modeling methods with the theoretical values of collision risk.

During the accuracy comparison process in this study, we merged the spatial scope of the ship domain into the spatial modeling results of the ship-encounter space domain to ensure that the collision risk is always 1 when the scale factor of the ship-encounter space domain is in the interval [0,0.5]. This aims to improve the visual comparison effect of the method. Subsequently, the fitting results of the scaling factor in the [0.5,1] interval were compared and analyzed. The comparison results indicate that in the [0.5,1] interval, the prediction results of the various spatial modeling and analysis methods were not very different from the fitting results of the theoretical values.

Figs. 29(a) and (b) present the simulation results of the spline and ordinary kriging (OK) methods and the fitting results of the theoretical values of collision risk. After careful comparison, the calculation effects of the spatial modeling and analysis methods of the spline method and the OK method are not obvious, and there are high deviations in some numerical intervals. Particularly, when the scale factor value of the ship-encounter space domain is in the [0.6,0.85] interval, the corresponding spatial modeling and analysis results deviate considerably, with deviation values reaching up to 0.12. Fig. 29(a) presents the fitting results of the spline method. Line segments of different colors in the figure represent the mathematical fitting results using different built-in parameters (ρ). The choice of different built-in parameters ρ has different effects on the convergence of the simulation results. For example, blue represents the spatial modeling and simulation using the built-in parameters of $\rho = 1$, while green represents the spatial modeling and simulation using the built-in parameters of $\rho = 2$. Fig. 29(b) shows the fitting result of the OK method, and the line segments of different colors indicate that different spatial variation functions (such as sphere, linear, and Gauss) are used for mathematical fitting. For example, the blue and green colors represent the use of the sphere spatial variation function for spatial modeling and simulation and the use of the linear spatial variation function for spatial modeling and simulation. The numerical fitting results show that the accuracy deviation between the spline method and the OK method is very likely to be related to the spatial variation function and built-in parameters selected in the method and may also have a greater relationship with the complexity and randomness of the spatial distribution of dangerous outcomes. When the ship collision risk is in the high-value range, i.e., the scaling factor value of the encounter space domain is in the [0.85,1] interval, the results of the spatial modeling and analysis of the spline method and the OK method are greatly improved. However, although the optimal built-in parameters and spatial variation function are chosen for spatial modeling and simulation, some deviations still exist in the simulation results. The impact of this error on the results cannot be ignored. On the other hand, the spatial modeling and analysis results of the method proposed in this study must be considered for the ship-encounter space domain. It consistently minimizes the difference in fitted values from theoretical values of encounter risks in all numerical intervals, and the convergence effect is also the best. The main reason is that the proposed method can flexibly and comprehensively consider the multiple attribute characteristics of the special results in encountering danger; the effect of the natural neighbor (NN) method is the second reason, with an overall error of ~0.04. Figs. 29(c) and 29(d) depict the simulation results of the NN method and proposed method as well as the fitting results of the theoretical values of encounter risks. Meanwhile, we presented the comparison results of the fitting accuracy between the proposed method and the other three methods in a more intuitive form. Fig. 30 shows the fitting accuracy results of the proposed method in detail compared to the other three methods. The fitting effect of the OK and spine methods is the worst, mainly due to significant deviation in the spatial modeling and analysis results within some numerical ranges (0.6–0.85). The proposed method exhibited the best fitting accuracy, reaching 98.2%. The NN effect is also acceptable, with an overall fitting accuracy of ~96.1%. Therefore, based on the comprehensive comparison results shown in Fig. 29, it can be concluded that the proposed method exhibits the best performance in spatial modeling and analysis of the risk degree in the ship-encounter space domain, enabling more precise and effective extraction of the spatial trend and distribution pattern of potential navigational hazards.

An error analysis was performed using the encounter-risk value between the evaluation point and its surrounding elements to assess the accuracy of the spatial modeling results in the ship-encounter space domain. The classical mean absolute error (MAE), root-mean-square error (RMSE), and mean relative error (MRE) were used as error analysis indices for collision risk interpolation. Generally, smaller values of MAE, RMSE, and MRE indicate smaller errors in the spatial modeling results and higher accuracy of the spatial modeling method. Furthermore, a value of R^2 closer to 1 indicates a closer match between the

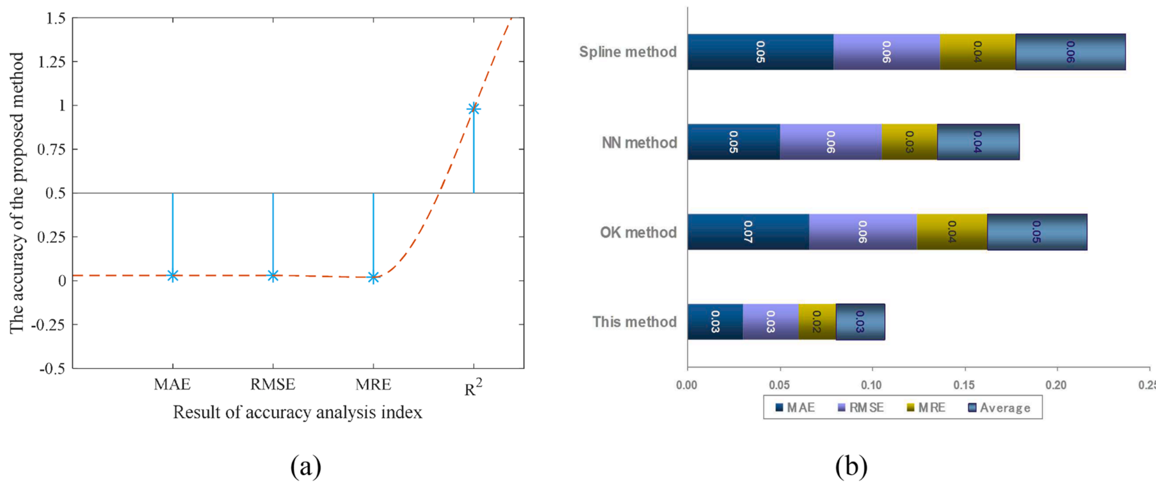

Fig. 31. Accuracy and comparison of the proposed method and other modeling methods: (a) accuracy of the proposed method; (b) comparison of the proposed method with other modeling methods.

Table 3
Error analysis index of the spatial modeling and analysis method for the ship-encounter space domain.

Error analysis index	Results of the error analysis index			
	Spline method	NN method	OK method	Accuracy of the proposed method
MAE	0.05	0.05	0.07	0.03
RMSE	0.06	0.06	0.06	0.03
MRE	0.04	0.03	0.04	0.02
Average	0.06	0.04	0.05	0.03
R^2	0.91	0.96	0.92	0.98

spatial modeling result and the theoretical value, indicating a better model. The error indicators were calculated using the following equations:

$$MAE = \frac{1}{n}\sum_{i=1}^{n}|\mu_r - \mu_e|, \tag{24}$$

$$MRE = \frac{1}{n}\sum_{i=1}^{n}\left|\frac{\mu_r - \mu_e}{\mu_r}\right|, \tag{25}$$

$$R^2 = 1 - \frac{\sum_{i=1}^{n}(\mu_r - \mu_e)^2}{\sum_{i=1}^{n}(\mu_r - \overline{\mu_r})^2}, \tag{26}$$

$$RMSE = \sqrt{\frac{1}{n}\sum_{i=1}^{n}(\mu_r - \mu_e)^2}, \tag{27}$$

where μ_r, $\overline{\mu_r}$, and μ_e represent the theoretical, theoretical average, and spatial modeling values of the encounter risk, respectively, and n denotes the number of evaluation points. Fig. 31(a) illustrates the accuracy of the proposed method in the ship-encounter space domain. The proposed method exhibited a low error rate and could accurately analyze and extract the spatial trends and distribution patterns of hazards in the multistate spatial–temporal ship-encounter space domain. This served to provide spatial analysis results that included the safety characteristics and temporal attribute information of the encounter for the safe navigation of ships, thereby improving the spatial perception and analysis of dangers in intelligent ship navigation.

Furthermore, we compared the accuracy of the proposed method with that of other modeling methods for ship-encounter space domains. The calculation and comparison results are presented in Fig. 31(b) and Table 3. The results indicate that the margin of error of the proposed method fluctuated between 0.2 and 0.3. The R^2 value was 0.98, which is only 2% away from 100%. The overall average error of the method in this study was ~0.03, whereas the accuracy of the other three methods was lower, as illustrated in Fig. 31(b), thus demonstrating the superiority and effectiveness of the proposed method.

4.4. Discussions and limitations

With the rapid development of intelligent navigation technology, the spatial analysis of navigational hazards has become a core problem that must be addressed. Traditional methods often struggle with the acquisition of sufficient nonlinear spatial distribution rules and spatial variation trend characteristics in the ship-encounter space domain. This study is oriented toward future research on intelligent navigation of ships and maritime traffic safety and proposes an innovative GIS modeling and analysis method for the spatial domain of ship encounters by taking advantage of the GIS spatial information platform. The proposed method enables in-depth analysis and perception of potential nonlinear spatial characteristics and distribution patterns of ship-encounter danger during ship navigation. Moreover, the proposed method performs GIS modeling and analysis in the ship-encounter space domain, allowing for extracting potential collision risk trends and spatial distribution pattern information in the ship-encounter space under multitemporal sequences and nonlinear spaces. This provides spatial analysis results that include encounter-safety features and spatial–temporal attribute information for safe ship navigation. As a result, the proposed method can greatly improve the ships' spatial analysis and perception of danger and effectively reduce the spatial ambiguity and uncertainty of danger.

To verify the effectiveness of the proposed method, simulations were performed, as described earlier in this section. The simulation examples consisted of two encounter scenarios with navigational hazards: one of a ship sailing with a turning-point route and the other of a ship sailing on a straight-line route. The proposed method successfully extracted the spatial distribution and change trends in the degree of collision risk and performed an in-depth analysis of potential nonlinear spatial characteristics and the distribution pattern of ship-encounter danger. Therefore, the GIS spatial modeling and analysis method proposed in this study can play an important role in extracting spatial information on potential ship-encounter hazards. In the application validation of the research example, spatial modeling and analysis of the ship-encounter space domain were performed for the two encounter scenarios, and the continuous spatial distribution information and spatial–temporal variation trend results of the potential navigation-encounter hazard

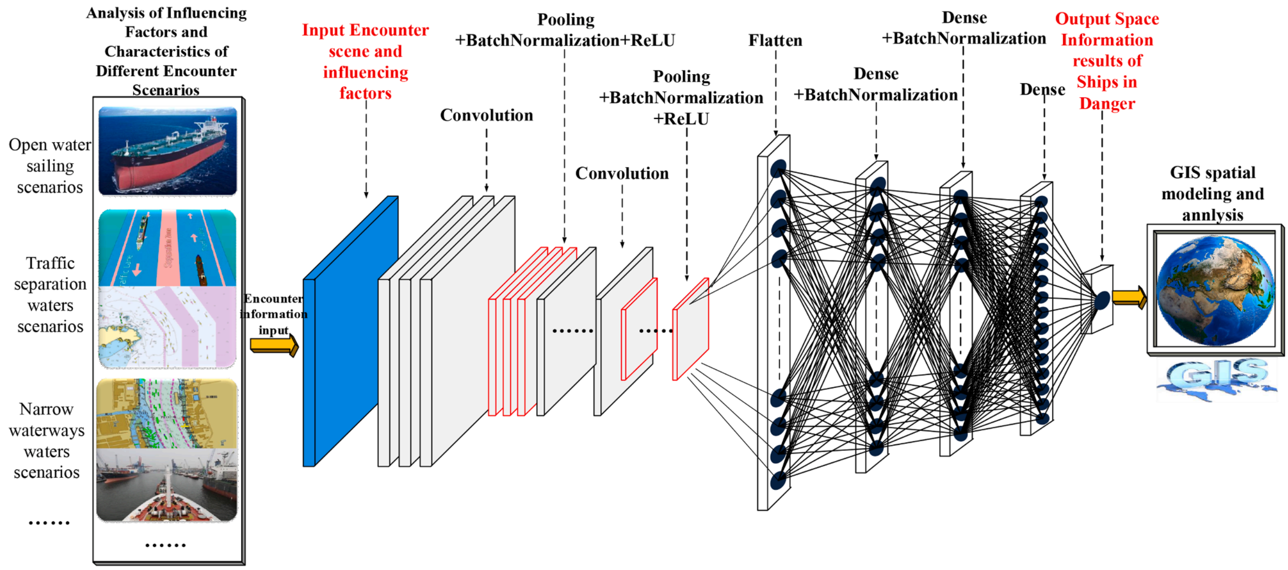

Fig. 32. Preliminary research concept of the safety analysis of ship encounters in various scenarios based on reinforcement learning.

degree were successfully obtained (Figs. 16 and 22). Furthermore, based on Moran's I index, we further analyzed and intuitively displayed the spatial–temporal heterogeneity and spatial homogeneity of the modeling results of the ship's local ship-encounter space domain. The results are provided in Figs. 21 and 25, which represent the spatial–temporal heterogeneity characteristics of the straight-line and turning-point route navigation scenarios, respectively. The modeling and analysis results of the ship-encounter space domain generally exhibited a spatial–temporal association pattern in which spatial units with high danger values were surrounded by spatial units with low danger values.

We conducted a time-series analysis of the modeling results of the ship-encounter space domain under the two navigation scenarios, and the results are provided in Figs. 19 and 24. The results are the time-series analysis results of the ship navigation scenarios, including the straight-line segment and turning-point route. The analysis results exhibited a similar trend to the change in the continuous spatial distribution of the encounter risk, indicating a phenomenon of high spatial risk near the center point. This phenomenon may be related to the fact that spatial distance is a dominant factor affecting the encounter risk.

Furthermore, we verified the accuracy of the simulation results of the proposed method using MAE, RMSE, MRE, and R^2, as discussed in Section 4.3, and compared it with that of the three other representative methods. The proposed method was found to be comparable to the other methods while exhibiting a higher accuracy. The accuracy comparison results are provided in Table 3. The comparison results reveal that the spline and OK methods had the worst effect on the modeling and analysis results of the ship-encounter space domain, with error values fluctuating between ~0.05 and 0.06. The NN method exhibited slightly better performance. In contrast, the comprehensive accuracy of the hazard spatial modeling results obtained by the proposed method was no less than 95%, with the highest accuracy reaching 98%. Therefore, the results of the simulation and comparative analysis of the simulation results demonstrate that the proposed method is highly accurate and effective. It can quickly and accurately reflect the potential nonlinear spatial characteristics and distribution pattern of ship collision risk according to the spatial modeling and analysis results of the ship-encounter space domain. Additionally, it can be effectively applied to the spatial feature perception analysis of the ship-encounter danger, leveraging the advantages of GIS spatial information analysis technology in navigation safety. It provides innovative theoretical support for the future development of intelligent ship navigation safety analysis technology.

In this study, we innovatively applied the concept of GIS spatial modeling and analysis to investigate intelligent ship navigation encounter safety and extracted rich and detailed spatial characteristics and distribution patterns information on ship-encounter danger. However, this study only tested the proposed method and verified its accuracy in a limited number of conventional encounter scenarios in open water. Therefore, in future research, we will further optimize and refine this method by combining real and continuous navigation tests, particularly addressing the shortcomings of the algorithm in complex and multiobstacle encounter scenarios. This will help enhance the stability and reliability of the proposed method.

5. Conclusions and future work

In this study, we propose a spatial modeling and analysis method for the ship-encounter space domain based on a spatial information platform and analysis technology for intelligent navigation safety. This method is based on the construction of a dynamic spatial–temporal model of ship encounters, which allows for in-depth analysis of potential nonlinear spatial characteristics and distribution patterns of ship-encounter danger during ship navigation. Moreover, the proposed method can extract the spatial trend information of potential collision risks in the ship-encounter space considering multitemporal sequences and nonlinear spaces. The proposed method provides rich and accurate ship-encounter spatial characteristic results and collision risk information for ship driving, reducing the spatial ambiguity and complexity of danger information during navigation. Further, we conducted an example analysis and comparative verification of the method using two ship-encounter scenarios. The results demonstrated the superiority and accuracy of the proposed method in extracting spatial information about ship-encounter dangers, greatly improving the ships' analysis of navigation safety. Continued research in this area can greatly improve the ability of spatial analysis technology to ensure intelligent navigation safety, thereby ensuring safer navigation.

In the next stage of our research, we will further apply GIS spatial modeling and analysis methods to the field of intelligent navigation safety analysis. Our goal is to extract richer and finer spatial characteristics and distribution patterns information on ship-encounter danger and provide effective methodological support for ship collision avoidance. While this study represents a preliminary attempt, there are still some limitations that need to be addressed in future research, which will

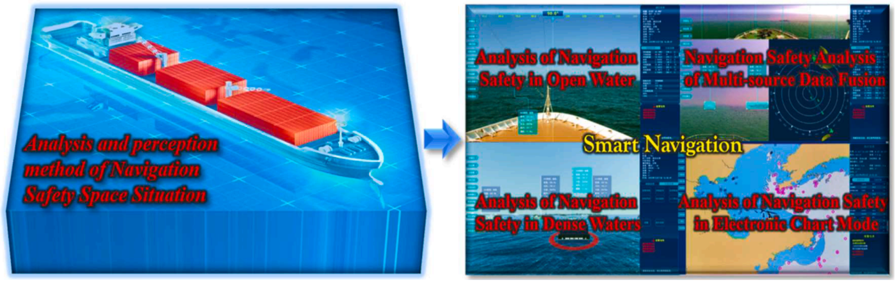

Fig. 33. Schematic of the intelligent navigation safety situation awareness and analysis system based on the geographic information system.

be conducted based on the following two aspects:

(1) In this study, we simulated and applied the proposed method using encounter scenarios in open water with navigational hazards as an example and obtained preliminary research results. However, in actual ship navigation, the navigation scenarios are complex and varied, including restricted waters, narrow waterways, traffic separation waters, and other navigation scenarios. These different scenarios require consideration of various factors when ships meet, including the navigation environment of the ship, the maneuverability of the ship, and avoidance paths. As a result, the design methods for the ship-encounter space domain will also differ and the calculation methods and steps for ship-encounter spatial analysis and modeling will vary.

To address these challenges, in the next research stage, we plan to use reinforcement learning to classify, calculate, and analyze dangerous situations encountered in various navigation scenarios. Fig. 32 illustrates the preliminary research concept of safety analysis of ship encounters in various scenarios based on reinforcement learning. The input information of the model consists of factors that affect the safety of ship encounters in different navigation scenarios. The reinforcement learning method can learn from the complex navigation state and the characteristics of a ship that encounters danger. Moreover, it can accurately evaluate and calculate the encounter safety of ships in different navigation scenarios through iterative calculation. An encounter-hazard assessment model covering all real navigation scenarios will be established to improve the reliability and authenticity of the research results. Continued research in this area can considerably improve the navigation perception and analysis capabilities of ships and provide model support for the future development of intelligent ship navigation and hazard analysis technology.

(1) In future research, we aim to enhance the spatial analysis theory of ship navigation safety based on the findings of this study. We plan to conduct a more comprehensive theoretical exploration of dangerous situations during ship navigation using a spatial information platform. We aim to further develop a GIS intelligent chart system that can facilitate autonomous ship navigation. This intelligent chart system will be based on a dedicated electronic navigation chart and will integrate multisource navigation environments and target data. This will help achieve more in-depth scientific exploration and mathematical optimization of the method for analyzing navigation space relations and hazard characteristic information. This system will apply to conventional navigation scenarios as well as other special navigation waters and states, providing the spatial analysis and mathematical methods required for different scenarios. The aim of the system is to achieve data integration, conversion, and sharing of navigation environment charts and navigation target information and to provide a new and advanced intelligent navigation spatial information platform with three-dimensional, high-precision, strong analysis, and precise extraction capabilities. This platform will provide ship drivers with space feature information and achieve intelligent navigation safety rapidly and accurately or more rapidly and accurately than using conventional methods. Fig. 33 provides a conceptual diagram of the GIS intelligent chart system, which can be used in the autonomous navigation of ships. Additionally, we plan to use the ocean-going teaching and research practice ship and an intelligent training ship (Fig. 34) owned by the school as well as the school-owned port connected to the Yellow Sea as a real ship test platform and navigation site for the implementation and theoretical verification of the proposed system.

CRediT authorship contribution statement

Zhichen Liu: Writing – review & editing, Writing – original draft, Visualization, Validation, Methodology. **Ying Li:** Resources, Writing – review & editing. **Zhaoyi Zhang:** Resources, Visualization. **Wenbo Yu:**

Fig. 34. Intelligent research and training navigation environment test platform for the testing and verification of the proposed intelligent navigation system.

Validation, Writing – review & editing. **Yegang Du:** Validation, Writing – review & editing.

Declaration of Competing Interest

The authors declare that they have no known competing financial interests or personal relationships that could have appeared to influence the work reported in this paper.

Data availability

Data will be made available on request.

Acknowledgments

This work is supported by National Key R&D Program of China (2021YFC2801000) and General Project of China Postdoctoral Science Foundation "Research on the Construction of Space Information Platform for Ship Encounter Safety Intelligent Nautical Chart under the S-100 Framework" (No. 2022M720625) and Open Fund of National Engineering Research Center of Ship & Shiping Control System" Research on Spatial Analysis Method of Intelligent Navigation Situation under Spatial Information Platform", and the development project of ship (navigation) situational intelligence perception system by the Ministry of Industry and Information Technology (No. MC-201920-X01).

References

[1] Zhang M, Zhang D, Fu S, Kujala P, Hirdaris S. A predictive analytics method for maritime traffic flow complexity estimation in inland waterways. Reliab Eng Syst Saf 2022:108317.
[2] The European Maritime Safety Agency. The annual overview of marine casualties and incidents. The European Maritime Safety Agency; 2022.
[3] IMO: MSC/Circ. 1029. Guidelines for formal safety assessment (FSA) for use in the imo rule-making process. London: IMO: MSC/Circ. 1029IMO; 2002.
[4] IMO. SFL 46/INF.5. development of revised SOLAS chapter II-I Parts A, B, and B-1: evaluation of required subdivision index r for passenger and dry cargo ship. Report from the HARDER Project. (2003-07-01).
[5] Coldwell TG. Marine traffic behavior in restricted waters. J Navig 1983;36:431–44. https://doi.org/10.1017/S0373463300039783.
[6] Zhao J, Wu Z, Wang F. Comments on ship domains. J Navig 1993;46:422–36.
[7] Zhaolin W, Zhongyi Z. Time collision risk and its model. J Dalian Marit Univ 2001; 02:1–5.
[8] Kearon J. Computer program for collision avoidance and track keeping. Proc. Int. Conf. Math. Aspects Marine Traffic. London 1977:229–42.
[9] Cai M, Zhang J, Zhang D, Yuan X, Soares CG. Collision risk analysis on ferry ships in the jiangsu section of the Yangtze river based on ais data. Reliab Eng Syst Saf 2021;215(2):107901.
[10] Zhang M, Montewka J, Manderbacka T, Kujala P, Hirdaris S. A big data analytics method for the evaluation of ship-ship collision risk reflecting hydrometeorological conditions. Reliab Eng Syst Saf 2021;213:107674. 2021.
[11] Silveira P, Teixeira AP, Figueira JR, Soares CG. A multicriteria outranking approach for ship collision risk assessment. Reliab Eng Syst Saf 2021;214:107789.
[12] Liu Z, Li Y, Zhang Z, Yu W. Spatial topological analysis model of ship encounter space. Ocean Eng 2020;202:107171. https://doi.org/10.1016/j. ocean eng.2020.107171.
[13] Fuji J, Tanaka K. Traffic capacity. J Navig 1971;24:543–52.
[14] Goodwin EM. A statistical study of ship domains. J Navig 1975;28:328–44.
[15] Szlapczynski R, Szlapczynska J. A ship domain-based model of collision risk for near-miss detection and collision alert systems. Reliab Eng Syst Saf 2021;214: 107766.
[16] Du L, Banda OAV, Huang Y, Goerlandt F, Kujala P, Zhang W. An empirical ship domain based on evasive maneuvers and perceived collision risk. Reliab Eng Syst Saf 2021;213:107752.
[17] Gil M. A concept of a critical safety area applicable for an obstacle-avoidance process for manned and autonomous ships. Reliab Eng Syst Saf 2021;214:107806.
[18] Montewka J, Manderbacka T, Ruponen P, Tompuri M, Gil M, Hirdaris S. Accident susceptibility index for a passenger ship-a framework and case study. Reliab Eng Syst Saf 2022;218:108145.
[19] Xin X, Liu K, Yang Z, Zhang J, Wu X. A probabilistic risk approach for the collision detection of multi-ships under spatiotemporal movement uncertainty. Reliab Eng Syst Saf 2021;215:107772.
[20] Hayama I. Evaluation method of collision risk by using true motion. Trans Nav Int J Mar Navig Saf Sea Transp 2017;11(1):65–70.
[21] Gil M. A concept of a critical safety area is applicable for an obstacle-avoidance process for manned and autonomous ships. Reliab Eng Syst Saf 2021;214:107806.
[22] Li M, Mou J, Chen P, et al. Toward real-time ship collision risk analysis: an improved R-TCR model considering target ship motion uncertainty. Reliab Eng Syst Saf 2022;226:108650.
[23] Pietrzykowski Z, Uriasz J. The ship domain-a criterion of navigational safety assessment in an open sea area. J Navig 2009;62:93–108. https://doi.org/10.1017/S0373463308005018.
[24] Pietrzykowski Z, Magaj J, Chomski J. A navigational decision support system for sea-going ships. Pomiary Autom Kontrola 2009;55:860–3.
[25] Pietrzykowski Z, Borkowski P, Wołejsza P. NAVDEC–navigational decision support system on a sea-going vessel. Zesz Nauk Akad Morska Szczecinie 2012;30:102–8.
[26] Wang S, Zhang Y, Zheng Y. Multi-ship encounter situation adaptive understanding by individual navigation intention inference. Ocean Eng 2021;237:109612. https://doi.org/10.1016/j. ocean eng.2020. 109612.
[27] Chen L, Yang P, Li S, et al. Online modeling and prediction of maritime autonomous surface ship maneuvering motion under ocean waves. Ocean Eng 2023;276:114183.
[28] Chen L, Yang P, Li S, et al. Grey-box identification modeling of ship maneuvering motion based on LS-SVM. Ocean Eng 2022;266:112957.
[29] Tavakoli S, Khojasteh D, Haghani M, et al. A review on the progress and research directions of ocean engineering. Ocean Eng 2023;272:113617.
[30] Zhang M, Conti F, Le Sourne H, et al. A method for the direct assessment of ship collision damage and flooding risk in real conditions. Ocean Eng 2021;237:109605.
[31] Goerlandt F, Montewka J. Maritime transportation risk analysis: review and analysis in light of some foundational issues. Reliab Eng Syst Saf 2015;138:115–34. b.
[32] Goerlandt F, Montewka J, Kuzmin V, Kujala P. A risk-informed ship collision alert system: framework and application. Saf Sci 2015;77:182–204. https://doi.org/10.1016/j.ssci.2015.03.015.
[33] Varas JM, Hirdaris S, Smith R, et al. MAXCMAS project: autonomous COLREGs compliant ship navigation. In: Proceedings of the 16th conference on computer applications and information technology in the maritime industries (COMPIT). 5; 2017. p. 454–64.
[34] Tian YF, Chen LJ, Huang LW, Mou JM. Featured risk evaluation of nautical navigational environment using a risk cloud model. J Mar Sci Technol 2018;19: 115–29. https://doi.org/10.1080/20464177.2018.1534929.
[35] Chen P, Huang Y, Mou J, Van Gelder P. Probabilistic risk analysis for ship-ship collision: state-of-the-art. Saf Sci 2019;117:108–22.
[36] Gil M, Montewka J, Krata P, et al. Determination of the dynamic critical maneuvering area in an encounter between two vessels: operation with negligible environmental disruption. Ocean Eng 2020;213:107709. https://doi.org/10.1016/j.oceaneng.2020.107709.
[37] Zhang W, Feng X, Goerlandt F, Liu Q. Towards a convolutional neural network model for classifying regional ship collision risk levels for waterway risk analysis. Reliab Eng Syst Saf 2020;204:107127.
[38] Du L, Goerlandt F, Kujala P. Review and analysis of methods for assessing maritime waterway risk based on non-accident critical events detected from AIS data. Reliab Eng Syst Saf 2020;200:106933.
[39] Dinis D, Teixeira AP, Soares CG. Probabilistic approach for characterising the static risk of ships using Bayesian networks. Reliab Eng Syst Saf 2020;203:107073.
[40] Liu Z, Li Y, Dong S, Zhang Z. Spatial logical relationship analysis model of ship encounter space. Ocean Eng 2021;239:109912.
[41] Abaei MM, Hekkenberg R, Bahoo TA. A multinomial process tree for reliability assessment of machinery in autonomous ships. Reliab Eng Syst Saf 2021;210: 107484.
[42] Yu Q, Teixeira ÂP, Liu K, Rong H, Soares CG. An integrated dynamic ship risk model based on Bayesian networks and evidential reasoning. Reliab Eng Syst Saf 2021;216:107993.
[43] Silveira P, Teixeira AP, Figueira JR. Guedes Soares C. A multicriteria outranking approach for ship collision risk assessment. Reliab Eng Syst Saf 2021;214:107789. https://doi.org/10.1016/j.ress.2021.107789.
[44] Zhang J, et al. An interpretable knowledge-based decision support method for ship collision avoidance using AIS data. Reliab Eng Syst Saf 2023;230.
[45] He Y, Liu X, Zhang K, et al. Dynamic adaptive intelligent navigation decision making method for multi-object situation in open water[J]. Ocean Eng 2022;253: 111238.
[46] Murray B, Perera LP. An AIS-based deep learning framework for regional ship behavior prediction. Reliab Eng Syst Saf 2021;215:107819.
[47] Zhang M, Montewka J, Manderbacka T, et al. A big data analytics method for the evaluation of ship-ship collision risk reflecting hydrometeorological conditions. Reliab Eng Syst Saf 2021;213:107674.
[48] Li M, Mou J, Chen L, He Y, Huang Y. A rule-aware time-varying conflict risk measure for mass considering maritime practice. Reliab Eng Syst Saf 2021;215: 107816.
[49] Zhu X, Xu H, Liu J. Domain and its model based on neural networks. J Navig 2021; 54:97–103.
[50] Zhang M, Kujala P, Hirdaris S. A machine learning method for the evaluation of ship grounding risk in real operational conditions. Reliab Eng Syst Saf 2022;226: 108697. https://doi.org/10.1016/j.ress.2022.108697.
[51] Montewka J, Manderbacka T, Ruponen P, et al. Accident susceptibility index for a passenger ship-a framework and case study. Reliab Eng Syst Saf 2022;218:108145.
[52] Zhang M, Zhang D, Fu S, et al. A predictive analytics method for maritime traffic flow complexity estimation in inland waterways. Reliab Eng Syst Saf 2022;220: 108317.
[53] Kim SJ, Taimuri G, Kujala P, Conti F, Le Sourne H, Pineau JP, Hirdaris S. Comparison of numerical approaches for structural response analysis of passenger ships in collisions and groundings. Mar Struct 2022;81:103125.

[54] Xu S, Kim E, Haugen S, Zhang M. A Bayesian network risk model for predicting ship besetting in ice during convoy operations along the Northern Sea Route. Reliab Eng Syst Saf 2022;223:108475.
[55] Mazurek J, Lu L, Krata P, Montewka J, Krata H, Kujala P. An updated method identifying collision-prone locations for ships. A case study for oil tankers navigating in the Gulf of Finland. Reliab Eng Syst Saf 2022;217:108024.
[56] Antão P, Sun S, Teixeira AP, et al. Quantitative assessment of ship collision risk influencing factors from worldwide accident and fleet data. Reliab Eng Syst Saf 2023;234:109166.
[57] Zhang J, Liu J, Hirdaris S, et al. An interpretable knowledge-based decision support method for ship collision avoidance using AIS data. Reliab Eng Syst Saf 2023;230:108919.
[58] Wenwen L, Yuanchang L, Richard B. Filtering based multi-sensor data fusion algorithm for a reliable unmanned surface vehicle navigation. J Mar Sci Technol 2023;22(2):67–83. https://doi.org/10.1080/20464177.2022.2031558.
[59] Zhang M, Taimuri G, Zhang J, Hirdaris S. A deep learning method for the prediction of 6-DoF ship motions in real conditions. Proc. Inst. Mech. Eng. Part M J. Eng. Marit. Environ. 2023. https://doi.org/10.1177/14750902231157852.
[60] Zhang Z, Li Y, Wu P, et al. An INS-aided MASS autonomous navigation algorithm considering virtual motion constraints and the leeway and drift angle. Ocean Eng 2023;272:113790.
[61] Szlapczynski R, Szlapczynska J. An analysis of domain-based ship collision risk parameters. Ocean Eng 2016;126(1):47–56.
[62] Zheng Z, Wu Z. Concept and model of ship collision risk in space. J Dalian Marit Univ 2001;1:1–4. +10.
[63] Liu Z, Li Y, Zhang Z, Yu W. A new evacuation accessibility analysis approach was based on spatial information. Reliab Eng Syst Saf 2022;222:108395.
[64] Chen C, Liu Y, Sun X, Di Cairano-Gilfedder C, Titmus S. An integrated deep learning-based approach for automobile maintenance prediction with GIS data. Reliab Eng Syst Saf 2021;216:107919. https://doi.org/10.1016/j.ress.2021.107919.
[65] Antonioni G, Bonvicini S, Spadoni G, Cozzani V. Development of a framework for the risk assessment of Na-Tech accidental events. Reliab Eng Syst Saf 2009;94(9):1442–50.
[66] Marsh PS, Frangopol DM. A reinforced concrete bridge deck reliability model incorporating temporal and spatial variations in probabilistic corrosion rate sensor data. Reliab Eng Syst Saf 2008;93(3):394–409. https://doi.org/10.1016/j.ress.2006.12.011.
[67] Rong H, Teixeira AP, Soares CG. Spatial correlation analysis of near-ship collision hotspots with local maritime traffic characteristics. Reliab Eng Syst Saf 2021;209(1):107463.